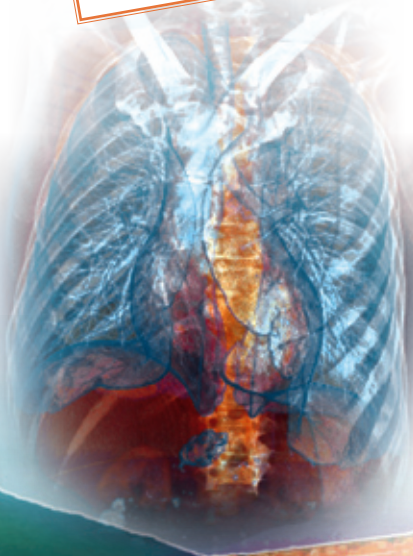


ESTI 2011

June 23-25, 2011
Heidelberg, Germany

Joint Meeting of ESTI and
The Fleischner Society

Innovation and
Education in
Chest Radiology



Abstract Book

www.ESTI2011.org



European Society of
Thoracic Imaging

EUROPEAN SOCIETY OF THORACIC IMAGING

THE FLEISCHNER SOCIETY





Oral Presentations

Functional imaging and therapy guidance in oncology

Thursday, June 23

14:15 – 15:45

Kopfklinik, Main Lecture Hall

O1

CT-guided marking of pulmonary malignant lesions with microcoil wires

Noeldge G.¹, Radeleff B.¹, Stampfl U.¹, Kauczor H.-U.¹

¹University Hospital Heidelberg, Diagnostic and Interventional Radiology, Heidelberg, Germany

Purpose: Thoroscopy is in many cases not the adequate access to extirpate non visible subpleural or deeper intrapulmonary localized malignant lesions in a lung parenchymal sparing manner. An alternative for the access to the lesion to be resected is offered by the CT guided marking with microcoil wires. The purpose of our study was the retrospective evaluation of the effectiveness of our first experiences with this method.

Material and method: A minimal invasive targeting at single or multiple lesions is offered by the CT -guided placement of microcoils into the lesions. This facilitates for the surgeon direct access to the lesion to be resected along the wire of the coil wire piercing through the skin after deployment. In our first group of patients with 6 males and 2 females, age between 8 and 58 years (mean: 26,4 years), mostly one, in one patient 3 malignant lesions were preoperatively marked.

Results: All 11 lesions could successfully be marked (100%). We had small pneumothoraces in 4/8 patients (50%); no treatment by thoracic drainages was needed. Lung parenchyma sparing extirpation of each lesion was successfully performed (100%). No major method related complications like arterial bleedings or parenchymal haematomas occurred. Histology revealed in all cases secondary lung tumors.

Conclusion: CT-guided marking with micro coil wire systems of single or multiple pulmonary lesions offers a direct, effective and safe pathway towards pulmonary lesions to be resected.

O2

Analysis of the clinical impact of chest digital tomosynthesis in the management of patients with suspected pulmonary lesions on chest radiography

Quaia E.¹, Baratella E.¹, Cioffi V.¹, Cernic S.¹, Lorusso A.¹, Casagrande F.¹, Cova M.A.¹

¹University of Trieste, Radiology, Trieste, Italy

Purpose: To assess the clinical impact of digital tomosynthesis (DT) in the management

of patients with suspected pulmonary lesions on chest x-ray radiography (CXR).

Materials and methods: Two-hundred-and-eighty-seven patients (173 male, 114 female; age, 70.82±11.2 years) with suspected pulmonary lesions after the initial analysis of CXR underwent DT. Two independent readers prospectively analyzed CXR and DT images and expressed a confidence score for each lesion (1 or 2: definitely or probably extra-pulmonary or pseudolesion; 3: doubtful lesion nature; 4 or 5: probably or definitely pulmonary). Patients did not undergo chest CT when DT did not confirm any pulmonary lesion (scores 1-2), or underwent chest CT when DT identified a definite non-calcific pulmonary lesion (scores 4-5) or was not conclusive (score 3). In patients who did not undergo chest CT the DT findings were confirmed by 6-12 months imaging follow-up. The time of hospitalization, and the mean image interpretation time for DT and CT were measured.

Results: DT identified a total number of 182 thoracic lesions, 127 pulmonary and 55 extra-pulmonary, in 159 patients while in the remaining 99 patients DT did not confirm any lesion. Chest CT was performed in 94/258 (36%) patients. The mean time of hospitalization was reduced from 2 weeks to 1 week. The mean interpretation time for DT (mean±SD, 200±40 secs) was higher ($P < .05$; Wilcoxon test) than for CXR (120±30 secs) but lower than chest CT (600±250 secs).

Conclusions: DT allowed to avoid chest CT in about two-third of patients with a suspected pulmonary lesions.

O3

Value of the computer-aided detection system in planning metastasectomy at chest CT: A prospective study in 50 patients

Goo J.M.¹, Kang C.H.¹, Kim Y.T.¹, Park C.M.¹, Lee H.J.¹

¹Seoul National University Hospital, Seoul, Korea, Republic of

Purpose: To evaluate the value of the computer-aided detection (CAD) system in the detection of pulmonary nodules at CT in patients who underwent metastasectomy.

Material/Methods: Fifty consecutive patients who underwent pulmonary metastasectomy were included in this study. CT scans with slice thicknesses of 1-1.25 mm were preoperatively performed, and then one chest radiologist identified the nodules initially through visual assessment followed by a review of the CAD marks. The locations of the nodules were annotated with numbers using PACS. These identifiers were used during surgical resection and pathologic evaluation.

Results: A total of 264 nodules (1-67 mm; median, 4 mm) were identified on CT; 222 through visual assessment and 42 additionally found with CAD (1-5 mm; mean 3 mm). Of the 264 nodules, pathologic results after surgical resection were available in 184 nodules, among which 115 were malignant (1-67 mm, median 9 mm). The 80 unresected nodules (1-7 mm, mean 3 mm) were similar in size to benign nodules (1-10 mm, mean 3 mm) ($p > 0.05$). Of the 42 nodules additionally detected with CAD, 28 nodules were not resected and 3 were malignant. An additional 15 nodules were resected in the surgical



field, of which 5 were malignant, but could not be localized on retrospective CT review.

Conclusion: Even in patients with primary extrapulmonary malignancy, 40% of surgically resected lung nodules were benign and 30% of nodules were not resected mainly due to their small size. CAD can help detect more nodules, but only 27% of resected nodules were malignant.

O4

In-vivo micro-CT / micro-PET imaging of lung adenocarcinoma in SPC-myc and SPC-raf transgenic mouse models

Rodt T.¹, von Falck C.¹, Halter R.², Boehm C.³, Glage S.⁴, Luepke M.³, Bortak J.², Wacker F.¹

¹Hannover Medical School, Diagnostic and Interventional Radiology, Hannover, Germany, ²Fraunhofer Institute for Toxicology and Experimental Medicine, Molecular Medicine and Medical Biotechnology, Hannover, Germany, ³University of Veterinary Medicine Hannover, General Radiology and Medical Physics, Hannover, Germany, ⁴Hannover Medical School, Laboratory Animal Science, Hannover, Germany

Purpose: SPC-raf and SPC-myc transgenic mouse models develop disseminated / circumscribed lung adenocarcinoma respectively, allowing assessment of carcinogenesis and treatment strategies. Micro-CT / micro-PET imaging findings, correlation to histology and technical considerations are addressed.

Material/Methods: More than 250 micro-CT and 40 ¹⁸F-FDG micro-PET of the chest were performed under inhalation anesthesia. Micro-CT / micro-PET registration was conducted using anatomical landmarks. Due to the diffuse and multifocal tumor growth in SPC-raf transgenic animals a quantification algorithm based on segmentation of the aerated lung areas as a surrogate was developed. To assess the individual tumor growth kinetics serial follow-up micro-CT was performed in a group of SPC-raf transgenic animals for more than 500 days. Applied radiation doses for different micro-CT protocols and micro-PET were measured using thermoluminescence dosimeters.

Results: An imaging routine for in-vivo assessment and quantification of lung tumor was established and evaluated. Autopsy and histology showed good correlation to imaging. Inter- / intra-observer variability of the quantification algorithm were 6.5% and 5.1%, respectively. The follow-up examinations depicted the tumor growth kinetics, resulting in a tumor ratio of >50% of the lung after 500 days. Mean micro-PET tumor-to-nontumor ratio was 2,55 for circumscribed lesions in SPC-myc transgenic animals. No significant correlation was detected between histological tumor load and tumor-to-nontumor ratio for diffuse tumors in SPC-raf transgenic animals.

Conclusion: In-vivo micro-CT / micro-PET imaging allows assessment and quantification of lung tumor load and growth in transgenic mouse models and can be used for evaluation of the models and therapy studies.

O5

Radiofrequency ablation of lung neoplasms in patients being no candidates for surgery. The impact of the intervention on the pulmonary function

Schneider T.¹, Puderbach M.², Bischoff A.², Kunz J.², Dienemann H.¹, Hoffmann H.¹, Thomas M.³, Herth F.J.F.⁴, Heussel C.P.²

¹Thoraxklinik, University of Heidelberg, Surgery, Heidelberg, Germany, ²Thoraxklinik, University of Heidelberg, Radiology, Heidelberg, Germany, ³Thoraxklinik, University of Heidelberg, Oncology, Heidelberg, Germany, ⁴Thoraxklinik, University of Heidelberg, Pneumology and Respiratory Critical Care Medicine, Heidelberg, Germany

Purpose: CT guided percutaneous Radio Frequency Ablation (RFA) of pulmonary lesions is an alternative option for patients being no candidates for surgery.

The pulmonary function should not be impaired substantially by the procedure.

In this study the pulmonary function subsequent to RFA of lung neoplasms as well as the morbidity related to the intervention was analyzed.

Methods: A total of 24 CT guided percutaneous RFA procedures were performed (in a total of 15 patients) after discussion in the national comprehensive cancer centre due to limited pulmonary reserve or other co-morbidities. Histology was proofed by CT-guided percutaneous biopsy (NSCLC: n=20; pulmonary metastasis: n=4) prior to the RFA procedure (in general anesthesia, double lumen intubation). Morbidity related to the intervention and the pulmonary function subsequent to the intervention was analyzed.

Results: The median forced expiratory volume (FEV1) pre RFA was 1.7l (range 0.7-2.9l; 65%, range 38%-129%). It was unchanged post RFA: 1.6l (range 1.1-2.4l; 64%, range 38%-118%) during median 168d follow-up (range 28- 393d). Pneumothorax requiring drainage as solely major complication occurred in 6/24 procedures (25%).

Median hospitalization time was 5 days (range 4-12 days). Local control by CT was reached in all cases; systemic disease progress was verified by PET in 3 patients.

Conclusions: Mid-term change in pulmonary function due to pulmonary RFA has a negligible clinical impact. Therefore RFA seems to be suitable especially in patients with severely limited pulmonary function, if other local strategies are unreasonable.

O6

Preoperative nodal staging in patients with non-small cell lung cancer: Comparison between multimodality MR imaging plus PET/CT and PET/CT alone

Yi C.A.¹, Lee K.S.¹, Kim Y.N.¹, Lee E.¹, Kwon O.J.², Kim B.-T.³, Kim S.W.⁴

¹Samsung Medical Center, Sungkyunkwan University School of Medicine, Radiology, Seoul, Korea, Republic of, ²Samsung Medical Center, Sungkyunkwan University School of Medicine, Pulmonology, Seoul, Korea, Republic of, ³Samsung Medical Center, Sungkyunkwan University School of Medicine, Nuclear Medicine, Seoul, Korea, Republic of, ⁴Samsung Medical Center, Sungkyunkwan University School of Medicine, Samsung Biomedical Research Institute, Seoul, Korea, Republic of



Purpose: To prospectively investigate the incremental value of multimodality MRI plus PET/CT compared with standard PET/CT alone for the preoperative nodal staging in patients with NSCLC.

Materials and methods: As a part of clinical randomized trial (NCT01065415), we consecutively included biopsy-proven NSCLC patients who were considered as operable on chest CT. They underwent multimodality MRI plus PET/CT, consisting of T2-weighted imaging, diffusion-weighted imaging (DWI), and PET/CT. Two group of readers blinded to each other evaluated each nodal station for the presence of metastasis with MRI plus PET/CT or PET/CT alone. Any nodal station which have metastatic features either on MRI or PET/CT were considered as metastasis in the interpretation of multimodality MRI plus PET/CT. Each nodal station's status was confirmed pathologically. The sensitivity (Ss), specificity (Sp), and accuracy (Ac) values of multimodality MRI plus PET/CT for nodal metastasis detection were evaluated on a per-nodal station basis, and compared with those of PET/CT alone by the use of McNemar test.

Results: In 49 patients (29 men and 20 women; range, 41-78; mean, 61.6 years), 39 (19%) of 206 nodal stations harbored malignant cells. The diagnostic efficacies (Ss 69%, Sp 93%, and Ac 89%) for detecting nodal metastasis were improved by adding DWI to PET/CT as compared with PET/CT alone (Ss 46%, Sp 96%, and Ac 87%) ($P = 0.003$, 0.062 , and 0.001 , respectively).

Conclusion: The combination of multimodality MRI and PET/CT helps to significantly improve the sensitivity and accuracy for detecting nodal metastasis in NSCLC patients as compared with PET/CT alone.

O7

Functional MR tools for diagnosing malignant pleural disease (MPD)

Coolen J.¹, De Keyzer F.¹, Nafteux P.², De Wever W.¹, Dooms C.³, Roebben I.¹, Vansteenkiste J.³, Verbeken E.⁴, De Leyn P.², Van Raemdonck D.², Decaluwé H.², Nackaerts K.³, Verschakelen J.¹, Dymarkowski S.¹

¹AZ Gasthuisberg, K.U. Leuven, Radiology, Leuven, Belgium, ²AZ Gasthuisberg, K.U. Leuven, Thoracic Surgery, Leuven, Belgium, ³AZ Gasthuisberg, K.U. Leuven, Pneumology, Leuven, Belgium, ⁴AZ Gasthuisberg, K.U. Leuven, Histopathology, Leuven, Belgium

Purpose: The aim of this study is to evaluate the potential role of diffusion weighted imaging (DWI) sequence in the differential diagnosis between benign and malignant pleural disease(MPD). Additionally, we examined if dynamic contrast-enhanced MRI (DCE-MRI) could further improve DWI-MR diagnostic value.

Material and methods: In 45 consecutive patients with pleural abnormalities suspect for MPD, who underwent a whole-body PET-CT, an additional MR with DWI- and DCE-MRI sequences were performed. Afterwards all patients underwent thoracoscopy with histopathological examination. DWI-MR was evaluated in a first step by calculating the apparent diffusion coefficient (ADC) of the suspect lesion; in case of equivocal values, interpretation of the curves derived from DCE-MRI data was the second step.

Both PET-CT and MR data were correlated with pathology.

Results: The sensitivity, specificity and accuracy of PET/CT for differentiating benign from MPD were 100%, 45.5% and 73.3%. The optimal ADC threshold to differentiate benign from MPD with DWI-MR was $0.00152 \text{ mm}^2/\text{s}$ giving a sensitivity, specificity and accuracy of 73.9%, 90.9% and 82.2% respectively.

This result could be improved to 87.0% ,86.4% and 86.7% respectively including DCE-MRI-data in case of ADC between 0.00152 and $0.00200 \text{ mm}^2/\text{s}$. In total 33 patients were staged correctly with PET-CT, 8 incorrectly and 4 undetermined. DWI staged 37 patients correctly and 8 incorrectly. Three of the four undetermined cases on PET-CT were correctly diagnosed on MRI.

Conclusion: DWI seems a robust tool for differentiation of benign pleural lesions from MPD. Accuracy of DWI can further improved by addition of DCE-MRI information.

O8

Iterative reconstruction for improving image quality of low radiation dose chest CT studies

Winklehner A.¹, Goetti R.¹, Frauenfelder T.¹, Alkadhi H.¹, BaumueLLer S.¹

¹University Hospital of Zurich, Institute of Diagnostic Radiology, Zurich, Switzerland

Purpose: To prospectively assess the impact of iterative reconstruction on image quality of low radiation dose chest CT.

Materials and methods: 20 consecutive patients (8 women, mean age 55 ± 21 y, BMI $24.9 \pm 4.5 \text{ kg}/\text{m}^2$, range 17.0 - $35.2 \text{ kg}/\text{m}^2$) underwent non-enhanced low radiation dose 64-slice CT of the chest (tube voltage 100kV, reference tube current-time product 30mAs, rotation time 0.5sec, pitch 0.6). Image data were reconstructed using the conventional reconstruction mode 'folded back-projection' (FBP) as well as a novel reconstruction approach called 'SAFIRE' (sinogram affirmed iterative reconstruction), which represents an iterative optimization process that reduces image noise using a noise modeling technique supported by raw data. Two blinded readers independently assessed quantitative (image noise) and qualitative image quality parameters (three-point scale; 1:excellent; 3:non-diagnostic) and identified each pulmonary abnormality in each MDCT dataset. Radiation dose parameters were recorded.

Results: Diagnostic image quality was present in 95%(19/20) of all patients when using FBP (25%(5/20) excellent, 70%(14/20) good, 0% non-diagnostic) and in 100%(20/20) of all patients when using SAFIRE (95%(19/20) excellent, 5%(1/20) good, 0% non-diagnostic). There was a significantly higher number of excellent image quality when using the SAFIRE reconstruction mode ($p < .001$). Mean noise was significantly lower for SAFIRE when compared to FBP ($31.5 \pm 4.9 \text{ HU}$ and $52.2 \pm 3.7 \text{ HU}$, respectively, $p < .001$). There were no significant differences regarding the overall depiction rate of pulmonary abnormalities ($p = .5$). Estimated effective radiation dose was $0.7 \pm 0.2 \text{ mSv}$, respectively.

Conclusion: Iterative reconstruction significantly improves image quality of low radiation dose chest CT and reliably enables the correct depiction of pulmonary abnormalities.



O9

Volumetric growth rate of 83 lung cancers screening detected: correlation with the metabolic activity and histological diagnosis

Rampinelli C.¹, Durlì I.¹, Lo Gullo R.¹, Raimondi S.¹, Veronesi G.¹, Bellomi M.¹

¹European Institute of Oncology, Milan, Italy

Purpose: To assess the correlation among the volumetric growth rate, the metabolic activity and the histology of 83 lung cancers screening detected in high risk population.

Materials and methods: Among the 186 lung cancers detected during 5-year low-dose CT screening, we retrospectively considered only the tumors for which a volumetric growth rate could be assessed between two or more CT scans and a preoperative 18-FDG PET/CT was available (n=83). For each cancer, at each CT scan, the semi-automated volumetry (mm³) and the Volume Doubling Time (VDT) were calculated using a dedicated software (LMS, Median Technologies). The SUV_{max}, the histology and the grading (G1-G3) were reported for each lung cancer. Associations of VDT with characteristics of tumors and patients were assessed with Spearman correlation coefficient, Kruskal-Wallis test and multivariate linear models.

Results: The mean VDT of the 83 lung cancers was 561 days (range: -261 to 4368 days); 48(57.8%) had a VDT < 400, 14(16.8%) had a 400 < VDT < 600 and 21(25.3%) had a VDT > 600 days. At the univariate analysis we found that VDT significantly decreased with increasing the SUV_{max} (p < 0.008), was significantly lower in adenocarcinomas compared to other histological types (p < 0.01) and in G1 tumors compared to G2/3 (p < 0.003). At the multivariate analysis only the association between VDT and grading remained significant (p=0.002).

Conclusions: We found that VDT was significantly associated with tumor grading. Our data suggested a possible association of VDT with histological type and SUV_{max}, although this seemed to be not independent by tumor grading.

Parenchymal and vascular applications

Thursday, June 23

16:00 – 18:00

Kopflinik, Main Lecture Hall

O10

Emergency radiology: Are we doing too many CTA studies for Pulmonary Embolism in low risk young patients?

Fernandez C.¹, Jimenez D.¹, Roma E.¹, Vilar J.¹

¹Hospital Doctor Peset, Radiology, Valencia, Spain

Purpose: To evaluate the diagnosis of Pulmonary Embolism (PE) in the young population in our emergency department in order to reduce CTA in low risk patients.

Materials and methods: We retrospectively analyzed the medical records of 52 patients under 50 years of age that underwent emergency CTA for suspected PE between January 2009 and November 2010. Low risk patients were selected applying the Pisa score. This low risk group was analyzed using the PERC rule. PERC was considered negative when none of the 8 criteria were met. The results of this triage were analyzed and compared with the clinical data, the D dimer and the CTA results. Statistical analysis performed included sensitivity, specificity, ROC curves and the Fisher's exact test.

Results: Out of 52 patients, 34 were low risk (65%), four of them had PE. Of the 34 low risk patients, 18 were PERC negative, and none had PE. More than 50% of the CTA studies could have been avoided. Twelve patients were PERC positive, and of these 4 had PE. PERC sensitivity and negative predictive value were 100%, specificity 60% and positive predictive value 25% with Fisher's exact probability of 0.04. The D dimer was positive in patients with negative PERC and negative CTA for PE.

Conclusions: PERC has a high negative predictive value in low risk patients less than 50 years. An appropriate clinical assessment can identify young patients that don't need CTA.

O11

Selfexpanding nitinol stents for the treatment of superior vena cava obstruction

Stampfl U.¹, Sommer C.-M.¹, Bellemann N.¹, Schellenberg M.², Heussel C.³, Thomas M.⁴, Kauczor H.-U.¹, Radeleff B.¹

¹University Hospital Heidelberg, Diagnostic and Interventional Radiology, Heidelberg, Germany, ²University Hospital Heidelberg, Pneumology and Respiratory Critical Care Medicine, Thoraxklinik, Heidelberg, Germany, ³University Hospital Heidelberg, Diagnostic and Interventional Radiology, Thoraxklinik, Heidelberg, Germany, ⁴University Hospital Heidelberg, Thoracic Oncology, Thoraxklinik, Heidelberg, Germany

Purpose: To retrospectively evaluate a new selfexpanding nitinol stent with closed-cell-design (Sinus XL, Optimed, Ettlingen, Germany) for the treatment of superior vena cava obstruction (SVCO) due to compression/infiltration by lung cancer.

Material and methods: Between 10/2009-10/2010, 10 patients (8 male, average age 62±10 years) suffering from stage IIIB (1 patient) or IV (9 patients) non-small cell lung cancer (NSCLC) and acute SVCO were scheduled for urgent stent implantation. Primary study endpoint was safety including accurate stent placement with complete coverage of the stenosis and complications. Secondary endpoint was efficacy.

Results: In the 10 patients 12 stents were implanted (stent diameter 20-26mm, length 40-60mm) via a combined transjugular/transfemoral venous approach. The stenosis in the vena cava superior could be completely covered in all patients (primary technical success 100%). Post-dilation was necessary in 5 cases (diameter 12-24mm). Stent dislocation immediately after deployment into the right atrium as occurred in a single patient, was successfully repositioned and stabilized by a second stent within the same intervention. The clinical symptoms of SVCO improved after stent implantation in all patients (mean follow-up was 92 days). In one patient, the stent occluded due to tumour



growth 44 days after stent implantation with recurrence of symptoms. In this patient, the stent was recanalized and a second stent was placed, however, pulmonary embolism occurred during the procedure, and the patient died one day after the procedure

Conclusion: The implantation of a selfexpanding nitinol stent for the treatment of SVCO is a safe and effective emergency treatment.

O12

Evaluation of HRCT findings and pulmonary function tests in rheumatoid arthritis patients after one year of treatment with anti-TNF agents

Detorakis E.E.¹, Raissaki M.¹, Magkanas E.¹, Voloudaki A.¹, Sidiropoulos P.², Boumpas D.²

¹University Hospital of Heraklion, Radiology, Heraklion, Greece,

²University Hospital of Heraklion, Rheumatology, Heraklion, Greece

Purpose: To evaluate the changes regarding chest HRCT and pulmonary function tests (PFT) after 1-year-treatment with anti-TNF agents in rheumatoid arthritis (RA) patients with interstitial lung disease (ILD).

Material/Methods: 22 consecutive patients, 10 males, 11 females, aged 23-76 years (mean 49.5) previously diagnosed (1-12 years, mean 6.5) with RA and with pre-existing RA-related-ILD were prospectively recruited. No patient had a history of smoking, asthma, COPD or pulmonary hypertension. Inspiratory and expiratory chest HRCT and PFT's were performed before and after 1-year-treatment with methotrexate combined with either infliximab or abatacept. HRCT images were evaluated and scored for ground glass opacities (GGO), nodules, reticulation, honeycombing, bronchiectasis/ bronchiolectasis and air trapping (AT) by two chest radiologists in consensus. Statistical evaluation was performed using paired-sample t-test, chi-square, Mann-Whitney and Spearman's correlation (SPSS 16.0); $p < 0.005$ was statistically significant.

Results: In the pre-treatment HRCT, reticular pattern was detected in 18 patients (81.8%), honeycombing in 5 (22.7%) GGO's in 4 (18.1%), nodules in 6 (27.2%), bronchiectasis in 13 (59%), bronchiolectasis in 4 (18.2%). In 10 patients (45.4%) air trapping was registered on expiration. Inspiratory lesions' extent between pre and post-treatment HRCT did not exhibit any statistically significant difference (13.1 ± 13.1 vs. 13.6 ± 15.7 , $p = 0.693$) while AT extent was significantly reduced (12.9 ± 13.4 vs. 11.9 ± 12.9 , $p = 0.042$). Inspiratory lesions' extent & AT extent did not correlate with PFT parameters. FEV1 and FEV1/FVC ratio were significantly reduced (86.1 vs. 78.8 , $p = 0.045$). The extent difference of inspiratory lesions correlated negatively with changes in forced vital capacity (FVC) ($\rho = -0.632$, $p = 0.002$).

Conclusion: Anti-TNF treatment doesn't influence inspiratory lesion extent but may be related to air trapping improvement, FEV1 and FEV1/FVC ratio reduction.

O13

Assessment of pulmonary haemodynamics in patients with chronic thromboembolic pulmonary hypertension (CTEPH) by high temporal resolution phase-contrast MR imaging

Wirth G.M.¹, Weber S.², Schneider J.¹, Mayer E.³, Düber C.¹, Kreitner K.-F.¹

¹Universitätsmedizin Mainz, Radiologie, Mainz, Germany, ²Universitätsmedizin Mainz, Physik, Mainz, Germany, ³Hildegardis Krankenhaus, Thoraxchirurgie, Mainz, Germany

Purpose: To assess pulmonary vascular resistance (PVR) and mean pulmonary artery pressure (mPAP) using high temporal resolution phase-contrast magnetic resonance imaging (PC-MRI) and to correlate these with simultaneous invasive catheter-based pressure measurement.

Material and methods: Nineteen patients with CTEPH underwent simultaneously acquired catheter-based pressure measurements and high temporal resolution PC-MRI (1.5T system). Using an unsegmented 2D-FLASH-sequence with high temporal resolution (TR/TE 10msec / 2.5msec), the measurements were performed with prospective ECG-triggering and during free breathing of the patients. Based on velocity- and flow-time-curves, the absolute acceleration time (Ata), the maximum of mean velocities (MV), the volume of acceleratin (AV) and the maximum flow acceleratin (dQ/dt) were calculated. The PVR was evaluated with the parameters: mPAP, cardiac output and a given left atrial pressure pressure of 10 mmHg.

Results: Using multiple correlation analysis a linear combination resulted in the following equation for calculation of mPAP: $\text{cmPAP} = 73.321 - (0.521 * \text{Ata}) - (0.628 * \text{MV}) + (1.755 * \text{AV}) + (0.002 * \text{dQ/dt})$. The derived values correlated very well with simultaneously measured invasive mPAP values ($R = 0.96$, $p < 0.001$). PVR was calculated by the following equation: $\text{cPVR} = (\text{cmPAP} - 10 \text{mmHg}) * 80 / \text{cardiac output}$. The PVR values were correlated with those values from right heart characterization resulting in a significant correlation ($R = 0.88$, $p = 0.001$).

Conclusions: High temporal resolution PC-MRI allows for reliable assessment pulmonary haemodynamics in patients with CTEPH. This result strengthens the role of MRI in the diagnostic work-up of the disease.

O14

Capability and limitations of multidetector Computed Tomography for detection and characterization of Pulmonary Hypertension

Dornia C.¹, Lange T.J.², Behrens G.³, Stiefel J.¹, Müller-Wille R.¹, Poschenrieder F.¹, Manos D.⁴, Pfeifer M.², Stroszczyński C.¹, Hamer O.W.¹

¹University Medical Center Regensburg, Department of Radiology, Regensburg, Germany,

²University Medical Center Regensburg, Department of Internal Medicine II, Regensburg, Germany, ³University Medical Center Regensburg, Department of Epidemiology

and Preventive Medicine, Regensburg, Germany, ⁴Dalhousie University, Department of Radiology, Halifax, Canada

Purpose: Right heart catheterization (RHC) is the reference for diagnosis of pulmonary hypertension (PH). However, multidetector computed tomography is of increasing importance in the diagnostic work-up of patients with PH. The aim of this study was to



evaluate the reliability of various CT parameters for diagnosing the presence and severity of PH.

Materials and methods: 172 patients who received RHC, chest CT and pulmonary function test within 3 months in the years 2003-2008 were included in this retrospective study. 114 (66%) were diagnosed with PH. The remaining 58 patients (34%) served as controls. PH-patients were grouped based on etiology according to WHO classification. Widest diameters of the main, left and right pulmonary artery (MPAD, LPAD, RPAD), ascending aorta (AA) and thoracic vertebra (VB) determined at the same level as MPAD were measured on CT.

Results: Patients with PH had significantly higher MPAD, RPAD, LPAD and MPAD/AA, MPAD/VB ratios than control subjects ($p < 0.001$). No significant differences within the PH subgroups were found. For MPAD ≥ 2.9 cm, ROC analysis showed a sensitivity of 93.9% and specificity of 62.1% for the presence of PH. Sensitivity and specificity for MPAD/AA > 1 was 63.2% and 93.1%, those for MPAD/VB 53.5% and 93.1%. The severity of PH did not correlate with CT parameters.

Conclusion: Easy to determine parameters on chest CT allow detection of PH independent of etiology of disease. In patients with dilated aorta, the vertebra can serve as alternative internal standard. Severity of PH cannot be estimated by CT parameters.

O15

Regional evaluation of lung emphysema in inspiratory and expiratory phases using new method for ventilation function using dynamic chest x-ray examination

Abe T.¹, Motohashi N.², Uema E.¹, Akiyama Y.¹, Shiraishi Y.³, Ogata H.², Ito M.¹, Kudou S.²
¹Institute of Japan Anti-Tuberculosis Association, Fukujiji Hospital, Clinical Radiology, Kiyose, Tokyo, Japan, ²Institute of Japan Anti-Tuberculosis Association, Fukujiji Hospital, Respiratory, Kiyose, Tokyo, Japan, ³Institute of Japan Anti-Tuberculosis Association, Fukujiji Hospital, Respiratory Surgery, Kiyose, Tokyo, Japan

Purpose: To evaluate the ventilation function of lung emphysema in inspiratory and expiratory phases using new method of dynamic chest x-ray examination.

Methods: 39 ventilation impairment patients with emphysema and 5 healthy volunteers were performed in this study. The institutional review board approval and written informed consent was obtained in all persons. The dynamic chest x-ray of the participants was obtained in the upright position in about 10 seconds of tidal breathing at rest, and these images were captured at 7.5 frames per second.

An automatic analyzing software for a ventilation function included as follow,

1. Lung fields extraction from dynamic chest X-ray.
2. Identification of small local areas.
3. Calculation of the maximal differential values in inspiratory and expiratory phases at the corresponding small local area in the series of dynamic chest X-ray.
4. Calculation of the regional inspiratory/expiratory flow-rate-ratio.

The average of the flow-rate-ratio was compared the patients with the healthy volunteers by using significant difference.

Results: The expiratory flow-rate was similar to inspiratory rate in healthy volunteers, and the average of inspiratory/expiratory flow-rate-ratio was 1.08 ± 0.07 (mean \pm S.D.). The expiratory flow-rate was smaller than inspiratory rate in patients with emphysema, and the average of the ratio was 1.20 ± 0.12 . The averages of those was significantly different between in the patients with emphysema and in the healthy volunteers in this study ($P = 0.0086$).

Conclusion: The inspiratory/expiratory flow-rate-ratio in patients with emphysema was larger than healthy volunteers. The new method for ventilation function has possibility to evaluate the flow-rate noninvasively.

O16

Black blood MRI predicts early mortality in patients with suspected pulmonary hypertension

Swift A.¹, Rajaram S.², Marshall H.³, Condliffe R.⁴, Capener D.³, Hill C.⁵, Davies C.⁵, Elliot C.⁴, Wild J.³, Kiely D.¹

¹Sheffield Cardiovascular Biomedical Research Unit, Sheffield, United Kingdom,

²University of Sheffield, Sheffield, United Kingdom, ³University of Sheffield, Sheffield,

United Kingdom, ⁴Sheffield Pulmonary Vascular Disease Unit, Sheffield, United Kingdom,

⁵Sheffield Teaching Hospitals NHS Trust, Sheffield, United Kingdom

Introduction: Double inversion recovery (DIR) 'black blood' MRI suppresses the signal from flowing blood providing accurate information on pulmonary vascular morphology in patients with pulmonary hypertension (PH). In addition slow flowing blood causes incomplete suppression resulting in pulmonary blood flow artefact (DIR-PFA). This study examines the prognostic value of a DIR-PFA scoring system in a mixed cohort of patients with PH.

Methods: DIR-MRI images for 233 patients referred with suspected PH who underwent right heart catheterisation (RHC) within 48 hours of the MR examination were reviewed. The degree of DIR-PFA was visually scored in all patients from 0-5 (0=absent, 1=segmental, 2=lobar, 3=distal main, 4=proximal main and 5=trunk). Pulmonary artery (PA), aorta (Ao), and PA main branch diameters were measured from which PA/Ao ratio and mean PA branch diameters (MAPB) were calculated. Prognostic importance was assessed using multiple forward stepwise Cox regression analysis and Kaplan-Meier analysis

Results: During a mean follow-up of 19 months, 35 patients died. DIR-PFA > 2.5 predicted mortality ($p=0.013$) and was demonstrated to be an independent imaging predictor of outcome ($p=0.009$). PA/Ao ratio, PA size, MPAB did not predict survival during the mean follow up for 19 months. DIR-PFA scoring was simple to perform with good inter-observer agreement ($k=0.83$).

Conclusion: DIR-PFA scoring in patients with suspected PH predicts early mortality.



O17

Chronic fibrotic sarcoidosis: HRCT morphology versus the composite physiological index as predictors of mortality.

Walsh S.L.¹, Sverzellati N.², Devaraj A.³, Wells A.U.¹, Hansell D.M.¹

¹Royal Brompton Hospital, Radiology, London, United Kingdom, ²Section of Radiology, Department of Clinical Sciences, University of Parma, Parma, Italy, ³St. Georges Hospital, Radiology, London, United Kingdom

Purpose: The prognostic role of HRCT is not well characterised in fibrotic sarcoidosis. The aim of this study is to identify prognostic HRCT patterns in patients with fibrotic pulmonary sarcoidosis and to ascertain if HRCT pattern scores are superior to the CPI in predicting outcome. Optimum thresholds for significant patterns and the CPI, which separate the group into prognostically distinct categories, are also evaluated.

Methods and materials: HRCT scans of 92 patients with fibrotic sarcoidosis were scored by two observers on the extent of abnormal lung and the proportions of fine and coarse reticulation, microcystic and macrocystic honeycombing and traction bronchiectasis. PFTs and the CPI were obtained from patient records. Using Cox proportional hazards analysis, HRCT patterns, PFTs including the CPI were evaluated. Optimum thresholds separating patients into prognostically distinct disease categories were identified for significant patterns and the CPI.

Results: HRCT features predictive of mortality on multivariate analysis were proportion of coarse reticulation (HR=1.02, CI=1.01-1.03, p = 0.03) and the CPI (HR 1.06, CI 1.02-1.10 p< 0.01). A CPI threshold of 50 units was identified as the strongest predictor of mortality (HR 6.56, CI 2.67-16.22, p< 0.0001).

Conclusion: In fibrotic sarcoidosis, HRCT features are weaker predictors of mortality than the CPI. A CPI threshold of 50 units separated patients into two prognostically distinct groups - those with limited disease and those with extensive disease. This prognostic distinction provides a rapid and clinically applicable tool for guiding management decisions.

O18

Connective tissue disease related fibrotic interstitial lung disease: a simple staging system

Walsh S.L.¹, Devaraj A.², Sverzellati N.³, Wells A.U.¹, Hansell D.M.¹

¹Royal Brompton Hospital, Radiology, London, United Kingdom, ²St. Georges Hospital, Radiology, London, United Kingdom, ³Section of Radiology, Department of Clinical Sciences, University of Parma, Parma, Italy

Purpose: The aim of this study was to devise a staging system based on imaging findings and physiological indices that separates patients with fibrotic interstitial lung disease across all connective tissue diseases (CTD-ILD) into two prognostically distinct

categories upon which dichotomous management decisions such as, 'amenable to therapy or not', may be based.

Methods and materials: 136 patients with a diagnosis of fibrotic CTD-ILD were identified. HRCT scans were scored by two observers on the extent of abnormal lung and the proportions of fine and coarse reticulation, microcystic and macrocystic honeycombing and traction bronchiectasis. Using Cox proportional hazards analysis, optimum thresholds separating patients into prognostically distinct 'limited' and 'extensive' disease categories were identified for fibrosis score, traction bronchiectasis and the CPI.

Results: Thresholds that provide optimal prognostic separation of the cohort were as follows; Fibrosis 50% (HR=5.3, CI= 2.2-12.8, p=0.0002), traction bronchiectasis (absent/present) (HR=5.1, CI= 1.6 -16.5, p=0.0002) and CPI 60 units (HR=2.4, CI=1.3-4.4, p=0.008). Combining these thresholds in an algorithm requiring an assessment of fibrosis with respect to a threshold of 50% with recourse to traction bronchiectasis and the CPI in indeterminate cases, a simple staging system was generated which separated the cohort into two prognostically distinct groups (HR 4.7, CI=0.9-24.4, p=0.0001).

Conclusion: Our results demonstrate the utility of a simple staging system that separates patients with fibrotic CTD-ILD into two prognostically distinct categories.

O19

Multi-Nuclear MRI Investigations into CF

Wild J.M.¹, Deppe M.¹, Ajraoui S.¹, Taylor C.J.²

¹University of Sheffield, Academic Radiology, Sheffield, United Kingdom, ²University of Sheffield, Institute of Child Health, Sheffield, United Kingdom

Introduction: The role of combined ³He functional and ¹H anatomical MRI in pediatric CF is reviewed with results from ³He ventilation, dynamic and gas washout studies and with anatomical ¹H MRI. Novel simultaneous multi-nuclear acquisition methods are evaluated for the acquisition of temporally registered fused ¹H/³He lung MRI. Examples of sensitivity to functional change post treatment are highlighted in a study of response to chest physio-therapy.

Methods: ³He ventilation, ³He dynamic, ³He washout and ¹H anatomical images were acquired from pediatric CF patients at 1.5T and 3T.

Results: ³He ventilation images visualised regional distributions that were shown to change pre and post therapy. Anatomical visualisation of mucus, bronchiectasis and lung fibrosis were visualised in the registered short TE ¹H MRI but the regional trends were not fully representative of those seen in ³He MRI. ³He washout imaging was shown to elucidate different temporal washout characteristics of ³He gas than is seen in healthy ventilated lung.

Discussion: ³He MRI has some additional sensitivity to changes in gas ventilation and exchange in early stage lung disease in CF that currently cannot be detected with ¹H MRI.



Conclusion: Multinuclear ^1H - ^3He MRI is a powerful functional imaging protocol with the potential to diagnose early stage lung disease and in the assessment of therapies in pediatric patients

Acknowledgements: Funded by UK EPSRC

O20

Inspiratory and expiratory MDCT (multidetector computed tomography) scans: automatic airways analysis in patients with chronic obstructive pulmonary disease (COPD)

Franchi P.¹, Amato M.¹, Larici A.R.¹, del Ciello A.¹, Roberta S.¹, Occhipinti M.¹, Contegiacomo A.¹, Bonomo L.¹

¹Catholic University, Bioimaging and Radiological Sciences, Roma, Italy

Purpose: To assess the role of MDCT with automated measurement of airways in the quantification of airflow obstruction in inspiratory and expiratory scans in patients with COPD.

Methods and materials: 20 patients with clinical diagnosis of COPD prospectively underwent pulmonary functional tests (PFTs) and chest CT scan. All CT exams were performed with a 64-rows scanner (slice thickness/interval 0.625 mm). Two consecutive acquisitions were obtained, one standard dose full inspiration scan followed by one low-dose (20 mAs) scan at the end of forced expiration. Datasets were analysed using an automated commercial software for airways analysis (Thoracic VCAR, GE Healthcare). One chest radiologist reported morphologic airway parameters, automatically calculated from lobar (second generation) to sub-subsegmental bronchi (fifth generation: diameter < 4 mm) on both inspiratory and expiratory scans: lumen diameter (LD), lumen area (LA), wall thickness (WT), wall area (WA), wall area ratio (WA%: wall area/total bronchial area%). Ratio between mean values of all automatic measurements obtained in inspiratory and expiratory scans were correlated with PFTs for each patient and each anatomic level (Pearson correlation coefficient).

Results: The best correlation ($p=0.04$; $p=0.08$) was observed between functional parameters of airflow obstruction (FEV_{1i} , $\text{FEV}_{1e}/\text{FVC}$) and the ratio between mean values of LA in expiration and mean values of LA in inspiration ($\text{LA}_{\text{exp}}/\text{LA}_{\text{insp}}$), at the level of the fifth bronchial generation.

Conclusion: Dynamic modifications of distal airways lumen area correlate with functional parameters indicative of airflow obstruction. MDCT with automatic measurement of the airway parameters may have a role in quantification of airflow obstruction in COPD patients.

O21

Comparative evaluation of chest radiography, low field MRI, the Shwachman-Kulczycki score and pulmonary function tests in patients with cystic fibrosis

Anjorin A.¹, Posselt H.-G.², Vogl T.J.³, Abolmaali N.⁴

¹University Hospital Heidelberg, Radiology, Heidelberg, Germany, ²University Hospital Frankfurt am Main, Paediatric Pulmonology, Frankfurt am Main, Germany, ³University Hospital Frankfurt am Main, Radiology, Frankfurt am Main, Germany,

⁴OncoRay - National Center for Radiation Research in Oncology, Dresden, Germany

Purpose: To evaluate comparability of Chrispin-Norman-Scores (CN) in patients with cystic fibrosis (CF) determined with conventional chest radiography (CXR) and fast low-field MR-imaging (MR) of the lung parenchyma.

Materials/Methods: 73 patients (age 7-32 years, median 14) with CF received their annual CXR and additional MR at 0.2T (Magnetom Open Viva, Siemens) using the breath-hold CISS-sequences (TR/TE=6.17/2.97ms, SL=20mm). In consensus reading two pediatric radiologists (AN, SH) with expertise in CF analyzed CXR and MR using the CN-Scoring system.

Results: The mean \pm standard deviation CN-score from MR was 12.0 ± 4.5 with a higher score than CXR in 23 patients (31.5%). The CN-Score from CXR was 12.1 ± 4.7 with a higher score than MR in 25 patients (34.3%). The difference between the two scores was 0.12 and was not significant. There was a significant correlation between both scores for all matched pairs ($p < 0.05$, $r = 0.97$). CXR and MR-CN-scores correlated better with the measured FEV1 ($p < 0.001$, $r = -0.65$) and ($p < 0.001$, $r = -0.65$) respectively than with FVC ($p < 0.001$, $r = -0.46$) and ($p < 0.001$, $r = -0.47$). Both scores correlated to some degree with the Schwachman-Kulczycki scores ($p < 0.001$, $r = -0.52$ for CXR and $r = -0.53$ for MR).

Conclusion: CN-scoring of CF is possible with fast low-field MR. Since scoring differences between CXR and MR are not significant, further research is strongly suggested to reduce radiation exposure in patients with CF in long term follow-up, especially in children with minor pulmonary involvement. In these cases the clinical scores are poor whereas the correlation of the imaging scores are high.

Posters

P22

Repeatability of MR imaging in chronic obstructive pulmonary disease (COPD)

Anjorin A.¹, Ley-Zaporozhan J.^{1,2}, Opgenorth A.¹, Sedlaczek O.¹, Kauczor H.-U.¹, Heussel C.-P.³, Ley S.^{1,2}

¹Universitätsklinik Heidelberg, Radiology, Heidelberg, Germany, ²University of Toronto, Medical Imaging, Toronto, Canada, ³Thoraxklinik, University of Heidelberg, Radiology, Heidelberg, Germany

Purpose: COPD is a broad disease entity defined by PFT, however providing only a global measure of the disease without being able to categorize subtypes. With the increasing number of therapeutic options, particularly when it is advanced, there is a high demand for a non-invasive imaging test to provide the regional information on structural



and functional changes in order to target therapies accordingly. Proton MRI of the lung was recently introduced into the clinical arena allowing for radiation free assessment of the above mentioned issues. So far, no data regarding the repeatability of this technique is available.

Materials/Methods: A comprehensive MR protocol (1.5T, Magnetom Avanto) was developed to investigate the different aspects of the disease. The protocol consisted of morphological, pulmonary perfusion, cardiac function and respiratory dynamics sequences. Overall, 9 patients (COPD stages III&IV) were investigated twice in a 24h interval.

Results: The mean examination time was 64min and all patients tolerated the examination well. Visual evaluation of morphological and perfusion sequences demonstrated a good repeatability of the visualization of the parenchymal loss and perfusion defects. Quantitative evaluation of flow measurements revealed considerable variations (interexamination difference for the PA flow: 7 - 64 ml). Evaluation of the respiratory dynamics showed a broad variation allowing for no meaningful interpretation.

Conclusions: The proposed imaging protocol is feasible and applicable even in significantly ill COPD patients. The protocol is easy to use and shows a high repeatability in the key aspects for assessment of morphological and functional disease components.

P23

Magnetic resonance imaging of mixed ground glass nodules

Koo C.W.¹, Chen Q.C.¹, Sigmund E.E.¹, Mcgorty K.¹, Mason D.M.¹, Naidich D.P.¹
¹New York University School of Medicine, New York, United States

Purpose: To evaluate mixed ground glass nodules (GGNs) utilizing 3 Tesla (T) MRI and 32-channel torso-array-coil and to correlate non-echo planar diffusion weighted imaging (DWI) and T2* measurements with pathologic findings.

Methods: Twelve patients with 13 GGNs > 1 cm in diameter detected on computed tomography were prospectively recruited for this Institutional Review Board approved study. T1-weighted 2D gradient echo (GRE), T2-weighted 2D turbo spin echo with fat saturation, T2*-weighted multiple GRE, and diffusion weighted single shot twice-refocused spin echo axial images of the GGNs were acquired at end inspiration without intravenous contrast. Apparent diffusion coefficient (ADC) and T2* values were determined and correlated to pathology.

Results: All GGNs were visualized with the T2-weighted 2D TSE sequence providing the best morphologic delineation. Pathology was available for 9 of 13 lesions. ADC ranged from 1.19 to 1.78 $\mu\text{m}^2/\text{ms}$ (mean 1.45 \pm 0.19) and T2* ranged from 6.78 to 27.81 $\mu\text{m}^2/\text{ms}$ (median 16.13, mean 16.68 \pm 7.19) for the 7 malignant lesions. ADC was 1.59 and 1.42 and T2* was 6.78 and 20.24 for the 2 malignant lesions with positive epidermal growth factor receptors. ADC ranged from 0.9 to 1.47 $\mu\text{m}^2/\text{ms}$ (mean 1.18 \pm 0.4) and T2* ranged from 6.87 to 10.93 (mean 8.9 \pm 2.87) for the 2 benign lesions.

Conclusion: 3T MRI with a 32-channel torso-array-coil provides a radiation free means

of GGN evaluation. The T2-weighted 2D TSE with fat saturation sequence yields the best lesion visibility. DWI and T2* measurements may provide quantitative measures for distinguishing malignant from benign nodules.

P24

Pulmonary CT findings in severe swine flu at a tertiary referral centre. Can radiological findings predict outcome?

Lazoura O.¹, Parthipun A.¹, Robertson B.¹, Downing K.¹, Finney S.¹, Padley S.¹
¹Royal Brompton Hospital, London, United Kingdom

Purpose: The utility of a semi-quantitative total lung disease (TLD) score derived from chest CT scans to predict clinical outcome has been demonstrated by Goodman et al in patients with ARDS. The purpose of this study is to derive a similar score for patients with severe swine flu admitted to intensive care unit (ICU) and determine if it can be used as a predictor of clinical outcome and requirement for extracorporeal membrane oxygenation (ECMO) treatment.

Materials and methods: Chest CT scans and clinical records of 33 ICU patients with severe H1N1 viral pneumonia were reviewed. The first chest CT scan performed in each case was assessed by two radiologists. The TLD score was calculated as the sum of consolidation and ground glass change area at three different levels (aortic arch, hila and 2cm above the diaphragm). Statistical correlation of this score to clinical outcome (survival or death) and necessity for ECMO treatment was performed.

Results: A statistically significant association was found between TLD score and requirement for ECMO treatment ($p=0.02$), but not between TLD score and patient outcome ($p=0.7$).

Conclusion: This study demonstrates that the TLD score in ICU swine flu patients is a useful predictor of ECMO treatment requirement. Since ECMO is reserved only for critically ill patients, this score may be used as a predictor for critical disease. Lack of correlation between TLD score and patient outcome in this study may be secondary to an inherent bias caused by the use of ECMO treatment.

P25

Volumetry of artificial lung nodules on 64-rows Computed Tomography (CT): precision of automatic vs semiautomatic method.

Calandriello L.¹, Larici A.R.¹, del Ciello A.¹, Cauro A.¹, Santoro S.¹, Ciresa M.¹, Amato M.¹, Bonomo L.¹
¹Catholic University of Rome, Department of Bioimaging and Radiological Sciences, Rome, Italy

To assess the precision of volumetry of artificial solid (S) and non solid (NS) lung nodules by using a tridimensional (3D) software equipped with full automatic and semiautomatic



methods. To assess the reproducibility of the semiautomatic volumetry. A chest phantom containing 28 artificial nodules (14 S, 14 NS) of known diameter and volume underwent 64-rows CT scan (slice thickness/interval 0.625 mm, lung kernel, 100 mAs, pitch 1.375). Nodules diameter ranged between 2.9-25.3 mm for S and 3.1-11.1 mm for NS. Two chest radiologists calculated the volume of each nodule independently in two reading sessions, 30 days apart, by using a 3D software equipped with full automatic and semiautomatic methods (Median LMS, Median Technologies). To assess the precision, standard deviation (SD) of the mean differences between the real and estimated volumes was calculated for each nodule with both methods. Inter- and intra-observer variability of semiautomatic volume measurements were also assessed by SD calculation.

Full automatic method of volume assessment has demonstrated higher variability for NS nodules (SD= ±62.5) than for S nodules (SD= ±5.9). Semiautomatic method has shown higher reproducibility in volume assessment for both S (SD = ±4) and NS (SD = ±7.6) nodules. A very low inter- and intra-observer variability (SD= ±0.2; SD= ±0.9) was reported for semiautomatic measurement of nodule volumes.

Semiautomatic volumetry of artificial lung nodules has proved to be more precise than the full automatic one, particularly for NS nodules. Semiautomatic volumetry has also demonstrated a very high inter- and intra-observer reproducibility in assessing nodule volume.

P26

MDCT in pediatric trauma of the lung

Ivkovic A.T.¹, Milosavljevic T.T.²

¹Clinical Center Nis, Center of Radiology, Nis, Serbia, ²ZC Vranje, Radiology, Vranje, Serbia

Pulmonary contusion, which occurs in 25-35% of all blunt chest traumas, is usually caused by the rapid deceleration that results when the moving chest strikes a fixed object. About 70% of cases result from motor vehicle collisions, most often when the chest strikes the inside of the car. Falls, assaults and sports injuries are other causes.

Purpose: The main aim is to show radiology signs of lung trauma in pediatric cases.

Material/Methods: We examined 184 child patients with signs of chest trauma. All patients were examined on 16 or 64 MDCT. Youngest patient was 9 months old. We used standard protocol with virtual bronchoscopy and MDCT pulmonary angiography.

Results: Most patients come after car accidents (138), rest of them after fall, bomb explosion, gas explosion, sport injury, assault with knife, bullet wounds, suicide attempt and bathroom accident. Lung injuries were blast or shock injuries with broken ribs or with penetration. We perform x-ray immediately after trauma but main reasons for CT were clinical signs. Unlike X-ray, CT scanning can detect the contusion almost immediately after the injury. We also performed ultrasound to find early pulmonary contusion. We measure type and the size of the injury to determine necessary for surgery.

Unlike older, child injuries were more often without fracture of the ribs but also more blast injuries. We also followed up injuries after 48 hours in cases without need for surgery.

Conclusion: CT is powerful tool for detecting of the pediatric lung trauma.

P27

Fully-automatic determination of the arterial input function for Dynamic Contrast-Enhanced Pulmonary MR Imaging (DCE-pMRI)

Kohlmann P.¹, Laue H.¹, Anjorin A.², Wolf U.³, Terekhov M.³, Krass S.¹, Peitgen H.-O.¹

¹Fraunhofer MEVIS - Institute for Medical Image Computing, Bremen, Germany, ²University Hospital Heidelberg, Department of Diagnostic and Interventional Radiology, Heidelberg, Germany, ³Johannes Gutenberg University Medical Center Mainz, Department of Radiology, Mainz, Germany

Purpose: Recent studies have shown that DCE-pMRI is a very appropriate imaging technique for the clinical assessment of lung diseases. For the quantitative analysis of pulmonary blood flow (PBF) an arterial input function (AIF) of the contrast agent entering the lung is required. This work presents a fully-automatic method to determine the AIF within the branching of the pulmonary trunk into the pulmonary arteries (BPA).

Material/Methods: In an ongoing study, 14 DCE-pMRI data sets from 7 male patients were acquired (6x chronic obstructive pulmonary diseases GOLD I-IV, 1x mild asthma, 50-76 years, 24h repeatability). Successive image-processing techniques enable the extraction of the pulmonary artery. Key components are the calculation of a temporal maximum-intensity-projection image, exclusion of unlikely regions considering baseline, time-to-peak, and peak enhancement, filtering operations, and connected components analysis. The BPA is detected by centerline extraction followed by graph analysis.

A circular or spherical region within the BPA encloses the voxels whose time courses define the AIF.

Results: The outlined method segmented the pulmonary artery in all data sets.

In some cases the segmentation mask contained the right ventricle, lobar arteries, and veins. However, the final steps of the proposed method correctly detected the BPA and subsequently the AIF in all cases.

Conclusions: This work eliminates the influence of a person who draws the AIF manually on the outcome of quantitative PBF analysis. Hence, a better comparability of longitudinal perfusion examinations and examinations of different patients is potentially enabled which will be investigated in a further study.

P28

Assessment of aortic arch calcification in digital tomosynthesis and chest radiography: A comparison with chest CT

Kim E.Y.¹, Kim Y.S.², Chung M.J.³, Lee K.S.³

¹Gachon University Gil Hospital, Department of Radiology, Incheon, Korea, Republic of,



²Gachon University Gil Hospital, Department of Internal Medicine, Incheon, Korea, Republic of, ³Samsung Medical Center, Sungkyunkwan University School of Medicine, Department of Radiology, Seoul, Korea, Republic of

Purpose: The aim of this study was to compare the diagnostic performance of digital tomosynthesis (DT) and radiography for the extent of aortic arch calcification (AAC) in asymptomatic out-patients using multidetector computed tomography (MDCT) as the reference method.

Material/Methods: The study included 100 asymptomatic out-patients who underwent MDCT; all patients underwent chest radiography and DT within one week from the CT examination. We evaluated the diagnostic performance and inter-observer agreement of DT and radiography for detection of the extent of AAC (four grades, 0-3) with MDCT as the reference standard. Grades of AAC on DT and radiography were also compared with calcium score based on MDCT.

Results: The mean CT calcium score was 559.5 (range = 7-3940) for a total of 50 patients who had AAC. On DT, overall accuracy for AAC was 93.5%, which was superior to that of radiography (overall accuracy is 70.5%) ($P < .01$). Inter-observer agreement was good for DT (kappa value = 0.74) and radiography (kappa value = 0.62) for diagnosis of AAC, and good for DT (kappa value = 0.64), and moderate for radiography (kappa value = 0.53) for evaluation of AAC grades. The overall correlation coefficient score between AAC grades on DT and CT calcium score was superior to that between AAC grades on radiography and CT calcium score (overall correlation coefficient score were 0.90 and 0.60, respectively).

Conclusion: Digital tomosynthesis is superior to radiography for detection of the extent of AAC.

P29

Free vs Forced: model-free characterization of ³He MRI dynamic lung ventilation measurements for different gas mixture application regimes

Terekhov M.¹, Gueldner M.², Gast K.¹, Wolf U.¹, Rivoire J.¹, Friedrich J.¹, Karpuk S.², Schreiber L.M.¹

¹University Medical Center Mainz, Radiology, Mainz, Germany, ²Johannes Gutenberg University Mainz, Institute of Physics, Mainz, Germany

Motivation: Dynamic ventilation (DV) of lung measured with ³He MRI is an efficient tool to study the intrapulmonary gas inflow. The common approach to data analysis is model function fitting of the signal-time curve. The parameters obtained by non-linear fit are ambiguous and dependent on the “tracheal input” determined by the applied bolus shape and volume. We performed the comparison of two ³He application regimes: bolus delivered by Application Unit (AU) in free breathing mode and 2) forced bolus inspiration from Tedlar bag (TB) via fine tube with high resistance. In analysis we suggest: 1) the ³He-signal in parenchyma is linearly connected with gas amount passed trachea 2) the

parenchyma gas transport is diffusive. Thus, the ³He-signal is described with “regional transport constant” simultaneously characterizing the rate and amount of ³He delivery. The analysis was performed on model-free bases using linear transfer function (LTF) which transforms the input bolus signal $S_i(t)$ into regional response $S_{out}(t)$.

Results and discussion: The results show that LTF-approach can be applied to characterize data of DV with ³He-MRI. The discrepancy between application modes in terms of LTF shows that “forced” TB-application leads to strong changes of gas transport in parenchyma in comparison with “free breath” (AU). The kinetic of ³He delivery for TB-mode could not be described by 1-st order LTF, probably because the high pressure gradient, required to overcome the resistance, leads to much higher velocity of gas in trachea and convective mechanism has stronger effect in parenchyma in comparison with AU-application.

P30

Magnetic resonance imaging (MRI) for detection of onset, progression and follow up of lung disease in infants and young children with cystic fibrosis (CF)

Sumkauskaitė M.¹, Fritzsching E.², Kopp-Schneider A.³, Obtazaitė D.-E.¹, Mall M.², Puderbach M.^{1,4}, Eichinger M.¹

¹German Cancer Research Center, Department of Radiology, Heidelberg, Germany,

²University of Heidelberg, Division of Pediatric Pulmonology and Cystic Fibrosis Centre,

Department of Pediatrics III, Heidelberg, Germany, ³German Cancer Research Center,

Department of Biostatistics, Heidelberg, Germany, ⁴Chest Clinics at University Hospital Heidelberg, Department of Diagnostic and Interventional Radiology, Heidelberg, Germany

Purpose: The onset and spontaneous progression of early cystic fibrosis (CF) lung disease is not well understood. The aim of the present study was to validate pulmonary MRI as a radiation-free, non-invasive imaging modality to study the onset and progression of lung disease in infants and young children with CF.

Materials and methods: In 34 CF patients (mean age: 2.3 (SD 1.7); 17f, 17m) MRI (1.5T) was performed in free breathing. For morphological imaging T2w-(HASTE PACE) and T1w T1-TSE sequences pre and post contrast media in coronal and transversal orientation were used. Functional measurements were performed with a 3D-FLASH-sequence with a temporal resolution of 1.5s after iv injection of Gadolinium-DTPA. Two independent radiologists analyzed the images using a dedicated MRI score (range 0-72).

Results: The mean global, morphology and function scores for readers 1/2 (range) were: 11,4 (0-28)/10,2 (1-24); 7,9 (0-20)/7,4 (0-17) and 3,6 (0-9)/3,2 (0-7). Morphological and functional abnormalities were detected by MRI in the first year of life (n=6), Score 6.3(SD 2.6) and the score increased to 16.2 (SD 3.8) at the age of 4 years (n=5). Global scores decreased from 20.4 (SD 9.0) to 13.0 (SD 7.6) after antibiotic therapy for pulmonary exacerbations (one reader, paired t-test, $p < 0.05$).

Conclusion: Our study indicates that MRI of the lung is sensitive for morphological and functional lung changes already in the first years of life, disease progression and response



to therapy in infants and young children with CF.

Supported by Mukoviszidose e.V.

P31

Novel 3D-visualization and reporting methods for oncologic thoracic CT scans.

Dicken V.¹, Birr S.², Stoecker C.¹, Geisler B.¹, Bornemann L.¹, Kuhnigk J.-M.¹, Moltz J.¹, Ritter F.¹, Krass S.¹, Preim B.², Peitgen H.-O.¹

¹Fraunhofer MEVIS, Bremen, Germany, ²University of Magdeburg, Computational Visualistics, Magdeburg, Germany

Purpose: To improve communication between radiology, oncology, thoracic surgery and possibly pathology on patients undergoing chemotherapy or considered for resection of pulmonary metastases a document format enabling interactive 3D-visualizations and user input was designed.

Materials/Methods: A pdf-document was implemented to present radiological information in an animated and structured way and to allow for 3D-viewing of segmented structures in the lungs and mediastinum without the need to employ dedicated software or special databases in the clinic. It uses results concerning detection of pulmonary nodules from a radiologist (possibly using CAD) on high-resolution CT-scans. Further semi-automated analysis of the lungs for computer recognition of airways, lobes and vasculature are used.

Results: The PDF format enables selective visualization of structures relevant to referring physicians. An overview 3D-rendering condenses most relevant oncologic information into one picture. Using interactive 3D-renderings it becomes possible to better understand the complex geometry of the diseased lung prior to surgery. An interactive lesion list allows easy identification of all reported findings to decide if resection is required and possible.

During evaluation with surgeons and radiologists the proposed document format was considered helpful to efficiently communicate findings and plan a resection. 3D-Visualizations may also improve communication with the patient and surgeons in training.

Conclusions: A partly editable document format allows more informed clinical decisions. It enables integrating intra-operative findings precisely to particular lesions. Specimens could be labeled according to the lesion list and pathology findings may thus reliably associated with radiological and surgical data on a per lesion basis.

P32

Ventilation- and perfusion-weighted MRI by Fourier decomposition: Validation with hyperpolarized ³He-MRI and dynamic contrast-enhanced MRI in porcine lung

Bauman G.¹, Scholz A.², Rivoire J.², Terekhov M.², Friedrich J.², de Oliveira A.³, Semmler W.⁴, Schreiber L.M.², Puderbach M.^{5,6}

¹German Cancer Research Center, Division of Medical Physics in Radiology, Heidelberg, Germany, ²Johannes Gutenberg University Medical Center, Department of Diagnostic and Interventional Radiology, Mainz, Germany, ³Siemens Healthcare, Erlangen, Germany, ⁴German Cancer Research Center, Medical Physics in Radiology, Heidelberg, Germany, ⁵German Cancer Research Center, Division of Radiology, Heidelberg, Germany, ⁶Chest Clinics at University Hospital Heidelberg, Diagnostic and Interventional Radiology, Heidelberg, Germany

Purpose: Validation of non-contrast-enhanced lung ventilation- and perfusion-weighted imaging based on Fourier decomposition magnetic resonance imaging (FD-MRI) with dynamic contrast-enhanced MRI (DCE-MRI) and hyperpolarized ³He-MRI in an animal experiment.

Materials and methods: The study was approved by the local ethics committee. Three healthy pigs were studied in a 1.5T MR-scanner using FD-MRI, DCE-MRI and ³He-MRI. The animals were artificially ventilated and anesthetized. For FD-MRI, the ventilation- and perfusion-weighted images were obtained by post-processing of time-resolved data acquired using an untriggered 2D balanced steady-state free-precession sequence (TR/TE/TA=1.9/0.8/116 ms, 3.33 images/s, FA=75°, ST=12 mm). For DCE-MRI acquisitions with a 3D+t FLASH sequence (TR/TE=1.8/0.8 ms, FA=19°, ST=5.5 mm) were performed simultaneously with the injection of a contrast agent. To acquire the ³He-MRI data, a spoiled gradient echo sequence (TR/TE=7.0/3.5 ms, FA=12°, ST=10 mm) and the administration of 200 ml hyperpolarized of ³He was used. The first part of each examination was performed in healthy pigs using all imaging techniques. Afterwards, a pulmonary embolism was created using a balloon catheter. The perfusion FD-MRI and DCE-MRI were repeated. Subsequently, an obstruction of a bronchus was induced, which followed with FD-MRI and ³He-MRI ventilation measurements.

Results: Images acquired using FD-MRI, ³He-MRI, DCE-MRI in all healthy animals before the catheterization procedure showed homogenous distribution of ventilation and perfusion. Furthermore, artificially induced defects were detected by all MR-imaging methods at identical anatomical locations.

Conclusion: We have shown the usefulness of FD-MRI as a promising, non-invasive and easily implementable technique for the assessment of changes in lung function.

P33

Lung ventilation/perfusion imaging: Comparison of non-contrast-enhanced Fourier decomposition MRI with SPECT/CT in an animal experiment

Hintze C.^{1,2}, Lützen U.³, Ullrich M.³, Gaaß T.^{4,5}, Dinkel J.², Elke G.⁶, Meybohm P.⁶, Frerichs I.⁶, Hoffmann B.¹, Borggreve J.¹, Knuth H.C.¹, Schupp J.¹, Prüm H.⁷, Eichinger M.², Puderbach M.^{2,8}, Biederer J.¹, Bauman G.^{4,9}



¹University Medical Center Schleswig-Holstein, Campus Kiel, Diagnostic Radiology, Kiel, Germany, ²German Cancer Research Center, Radiology E010, Heidelberg, Germany, ³University Medical Center Schleswig-Holstein, Campus Kiel, Nuclear Medicine, Kiel, Germany, ⁴German Cancer Research Center, Medical Physics in Radiology E020, Heidelberg, Germany, ⁵Technical University Munich, Institute of Medical Engineering, Munich, Germany, ⁶University Medical Center Schleswig-Holstein, Campus Kiel, Anaesthesiology and Intensive Care Medicine, Kiel, Germany, ⁷German Cancer Research Center, Software Development for Integrated Diagnostics and Therapy Group, Heidelberg, Germany, ⁸Thoraxklinik Heidelberg, Diagnostic and Interventional Radiology, Heidelberg, Germany, ⁹University of Heidelberg, Computer Assisted Clinical Medicine, Mannheim, Germany

Purpose: Non-contrast-enhanced Fourier decomposition magnetic resonance imaging (FD-MRI) for ventilation- and perfusion-weighted imaging is compared to the clinical gold-standard of single photon emission computed tomography/computed tomography (SPECT/CT) in an animal experiment.

Material/Methods: The study was approved by the local animal care committee. Seven anaesthetized mechanically-ventilated pigs were examined by a 1.5T MR scanner and with SPECT/CT (MAGNETOM Avanto and Symbia T, Siemens AG, Healthcare Sector, Erlangen, Germany). Ventilation- and perfusion-weighted (Vw/Qw) imaging was acquired by post processing of an untriggered, two-dimensional balanced steady-state free-precession (bSSFP) sequence (TR/TE/TA=1.9/0.8/118 ms, 3.33 images/s, FA=75°, ST=12 mm, matrix=128x128). After a non-rigid image registration for elimination of breathing motion, the parenchymal signal intensity was analyzed pixel-wise with FD to separate periodic changes of proton density caused by respiration and blood flow. Spectral analysis was used to calculate V/Q-weighted images. Subsequently V/Q-SPECT was acquired after inhalation of dispersed ^{99m}Tc and injection of ^{99m}Tc macroaggregated albumin (MAA). Vw/Qw- and V/Q-images were reformatted into the same orientation for a ROI-based slice-wise analysis.

Results: Both modalities showed a homogeneous distribution of pulmonary V/Q and Vw/Qw, respectively. The gravitation dependent signal decrease in the upper lung sections in supine position was observed in FD-MRI and SPECT alike.

Conclusion: Vw/Qw-imaging by FD-MRI is comparable to V/Q-SPECT. Gravitation dependent signal changes can be monitored with both modalities. FD-MRI has the potential to be a radiation and contrast media free alternative to the clinical gold-standard of szintigraphy and SPECT.

P34

What is the best quantitative Computed Tomographic (CT) air trapping method that corrects for emphysema severity?

Mets O.M.¹, Zanen P.², Lammers J.W.J.², Isgum I.³, Gietema H.A.¹, van Ginneken B.^{3,4}, Prokop M.^{1,5}, de Jong P.A.¹

¹University Medical Center Utrecht, Radiology, Utrecht, Netherlands, ²University Medical Center Utrecht, Pulmonology, Utrecht, Netherlands, ³University Medical Center Utrecht, Image Sciences Institute, Utrecht, Netherlands, ⁴Radboud University Nijmegen Medical Center, Diagnostic Image Analysis Group, Nijmegen, Netherlands, ⁵Radboud University Nijmegen Medical Center, Radiology, Nijmegen, Netherlands

Background: Small airways disease and pulmonary emphysema are major components of chronic obstructive pulmonary disease (COPD). The best quantitative CT air trapping method that corrects for emphysema severity has not been established yet. In vivo quantification of these components may prove important in automated identification and phenotyping of COPD patients.

Objective: To compare quantitative CT air trapping measures that correct for emphysema in a population of lung cancer screening trial participants, by using the residual volume over total lung capacity ratio (RV/TLC), a widely used functional measure of air trapping, as reference test.

Methods: In 447 current or former heavy smokers participating in a lung cancer screening trial volumetric inspiratory-expiratory CT and lung function tests were obtained. We calculated the previously published methods of relative inspiratory to expiratory volume change between -860HU to -950HU (RVC_{-860to-950}) and expiratory to inspiratory ratio of mean lung density (E/I-ratio_{MLD}), and tested a third method (percentage of voxels between -780HU and -910HU in expiration; EXP_{-780to-910}). The RVC_{-860to-950}, E/I-ratio_{MLD} and EXP_{-780to-910} were compared with ROC analysis with RV/TLC as reference standard.

Results: The expiratory to inspiratory ratio of mean lung density (E/I-ratio_{MLD}) showed an AUC (95% CI) of 0.84 (0.81-0.88). This AUC was significantly higher than RVC_{-860to-950} (AUC= 0.70, p< 0.001) and EXP_{-780to-910} (AUC= 0.81, p=0.03).

Conclusion: The expiratory to inspiratory ratio of mean lung density in CT scans is the optimal quantitative method of air trapping detection in a population of current or former heavy smokers. This measure may prove important in future COPD research.

P35

To what extent can Computed Tomographic (CT) quantification of air trapping and emphysema explain airflow limitation in Chronic Obstructive Pulmonary Disease (COPD)?

Mets O.M.¹, Murphy K.², Zanen P.³, Gietema H.A.¹, Lammers J.W.J.³, van Ginneken B.^{2,4}, Prokop M.^{1,5}, de Jong P.A.¹

¹University Medical Centre Utrecht, Radiology, Utrecht, Netherlands, ²University Medical Center Utrecht, Image Sciences Institute, Utrecht, Netherlands, ³University Medical Center Utrecht, Pulmonology, Utrecht, Netherlands, ⁴Radboud University Nijmegen Medical Center, Diagnostic Image Analysis Group, Nijmegen, Netherlands, ⁵Radboud University Nijmegen Medical Center, Radiology, Nijmegen, Netherlands

Background: Both emphysema and small airways disease contribute to airflow



limitation in COPD. It has not yet been reported how well the combination of quantitative CT measurements of both components can explain lung function variance.

Objective: To determine to what extent the combination of quantitative CT measurements of air trapping and emphysema explains airflow obstruction in a population that covers the total spectrum of airflow limitation.

Methods: CT emphysema [2 methods: percentage inspiratory voxels < -950HU, (IN_{-950}); 15th percentile of attenuation curve, ($Perc_{15}$)] and CT air trapping [4 methods: percentage expiratory voxels < -850HU (EXP_{-850}); percentage expiratory voxels between -850HU and -910HU, ($EXP_{-850to-910}$); relative inspiratory to expiratory volume change between -860HU and -950HU, ($RVC_{-860to-950}$); expiratory to inspiratory ratio of mean lung density, ($E/I-ratio_{MLD}$)] were quantified on paired inspiratory and end-expiratory CT scans in 248 subjects (50 without COPD; 198 GOLD 1-4). The quantitative CT measurements were related to lung function parameters with univariate and multivariate linear regression analysis.

Results: In our cohort quantitative CT measurements of emphysema and air trapping showed good relationship to lung function parameters (univariate R-square up to 0.72). In multivariate analysis (corrected for sex, age and height) the combination of CT emphysema and CT air trapping explained 68-83% of the variance in airflow obstruction.

Conclusion: The combination of quantitative CT air trapping and emphysema measurements is strongly associated with lung function impairment, and explains a large part of the variance in airflow obstruction. Our results may prove useful in automated detection and phenotyping of COPD cases.

P36

Proper evaluation of thrombi, cysts and effusions using phase-sensitive inversion recovery

Tóth A.¹, Vágó H.¹, Takács P.¹, Balázs G.¹, Simor T.², Hüttl K.¹, Merkely B.¹

¹Semmelweis University, Heart Center, Budapest, Hungary, ²University of Pécs, Heart Institute, Pécs, Hungary

Purpose: Thrombi, effusions and cysts usually have long relaxation times. On images captured with inversion times (TI) used for late enhancement (LE) imaging these abnormalities will show up as a high intensity region. That is caused by the way negative magnetisation is reconstructed on magnitude images. There are several possibilities to aid the imaging physician in a more precise characterisation of these lesions. The simplest way is to increase the TI. However that requires a repeated scan. Alternatively there are sequences available nowadays on many commercial scanners to achieve that without lengthening the exam. Our goal was to demonstrate the usefulness of Phase-Sensitive Inversion Recovery (PSIR) for evaluating long T1 species, verified using the Look-Locker (LL) technique.

Methods: 1.5T Philips Achieva imaging instrument was used for acquisition.

Ten patients with left ventricular thrombi were included, three patient had pericardial

effusion and five having cyst were reviewed.

Results: LE dataset was available for all examinations. LL sequence didn't cover the lesion in eight cases. PSIR was enabled for all LE scans. The PSIR technique enabled us to identify the negative magnetisation suggesting false LE in all cases.

Conclusion: PSIR method can be applied in case of characterising thrombi and fluid containing abnormalities around the heart without time penalty. Optionally the LL sequence takes a single breath-hold only. It is beneficial to use these technical options in case it is available on the scanner to achieve more precise tissue characterisation.

P37

Management of pulmonary vein stenosis, a multiple and recurrent complication of catheter ablation for refractory atrial fibrillation. Five cases review. Single centre experience

Balázs G.¹, Kudrnova S.¹, Apor A.², Hüttl K.¹, Merkely B.², Vágó H.², Gellér L.²

¹Semmelweis University Heart Centre, Diagnostic and Interventional Radiology, Budapest, Hungary, ²Semmelweis University Heart Centre, Cardiology, Budapest, Hungary

Purpose: RFA of ectopic foci within pulmonary veins and surrounding atrial tissue represents effective treatment for AF. PVS constitutes its rare, but serious complication that may cause hemodynamic compromise leading to chronic irreversible vascular and parenchymal pulmonary changes. It occurs in 1-3% of mostly reablated patients even in very experienced centers. Along their variable presentation and unpredictable clinical course, the lesions are usually multifocal, multiple stenoses over 60% symptomatic. Although controversy exists in PVS management, MSCTA has been accepted as most reliable method of lesion's visualization, quantification and pulmonary vasculature and parenchyma monitoring. Endovascular balloon dilation and stent placement in occlusions and complex lesions presently offer most effective treatment with 57% restenosis rate. Through our centre's experience with iatrogenic PVS we would like to contribute to its management optimization.

Methods and materials: Since the introduction of catheter PV isolation in our centre in 2004, over 400 patients have been ablated and followed-up. 5 patients (3 reablated) have returned with PVS symptoms (effort dyspnoea, cough, hemoptoe). All the lesions were depicted by MSCTA or MRA and successfully endovascularly treated with immediate relief of symptoms and correction of pressure gradients.

Results: The PVS symptoms recurred and were acutely percutaneously treated in 3 patients (4 and 3 times in a single patient, 2-9 months following the previous treatment). We performed 10 successful interventional sessions, without complications.

Conclusion: Close post-ablation monitoring, early recognition of symptoms, prompt intervention in critical stenoses (primary stenting of complex lesions) are crucial for effective management of this chronic disease.



P38

Comparative measurement of bronchial wall thickness in non-enhanced and contrast-enhanced Multi detector row CT

Dettmer S.¹, Entrup J.¹, Schmidt M.², Wacker F.¹, Shin H.-O.¹

¹Medical School Hannover, Institute of Diagnostic and interventional Radiology, Hannover, Germany, ²Fraunhofer MEVIS, Bremen, Germany

Purpose: To evaluate potential variations of bronchial wall thickness measurements depending on application of intravenous contrast agent.

Materials and methods: Our study population consisted of 22 patients with suspected thoracic aortic dissection referred to CT angiography. They had no known pulmonary disorders. A non-enhanced CT scan of the chest was followed by a contrast-enhanced scan in the arterial phase (120 kV, collimation 32 x 1,25mm, reconstruction interval of 1 mm, standard reconstruction kernel, and 80 ml Imeron 350 at 4 ml /sec). The bronchial wall was measured with dedicated software (MeVis Airway Examiner) up to the level of the 4th generation bronchus in the left upper and the right lower lobe. Statistical analysis included a paired t-test comparing the bronchial wall thickness in non-enhanced and contrast-enhanced scans and evaluation of potential influencing co-factors (upper lobe vs. lower lobe, generation of bronchus...).

Results: Bronchial wall thickness was significantly different in non-enhanced and contrast-enhanced CT ($p < 0,01$). With increasing bronchial generation the wall thickness decreased while the difference in measurements remained stable in non-enhanced and contrast-enhanced scans independent of bronchial size (average difference in bronchial wall thickness: 0.1 mm). There were no statistically significant co-factors influencing bronchial wall measurements.

Conclusions: There were statistical significant differences in bronchial wall measurements in non-enhanced and contrast enhanced CT scans. These differences were constant with varying bronchial size showing that the differences in measurements were independent of bronchial generation. For measurements of the bronchial wall thickness, a standardized application of intravenous contrast agent is recommended.

P39

Lobar emphysema distribution in different severity stages of COPD.

Owsijewitsch M.^{1,2}, Ley-Zaporozhan J.¹, Berger D.², Kuhnigk J.-M.³, Heussel C.P.⁴, Herth F.J.⁵, Ley S.¹, Kauczor H.-U.¹

¹University Clinic Heidelberg, Department of Radiology, Heidelberg, Germany, ²German Cancer Research Center, Department of Radiology, Heidelberg, Germany, ³Fraunhofer MEVIS - Institute for Medical Image Computing, Bremen, Germany, ⁴Thoraxklinik, University of Heidelberg, Department of Radiology, Heidelberg, Germany, ⁵Thoraxklinik, University of Heidelberg, Department of Pneumology and Respiratory Care Medicine, Heidelberg, Germany

Purpose: To evaluate the lobar distribution of emphysema in different severity stages of COPD.

Materials and methods: 1306 subjects (at risk for COPD - 1096, GOLD stage 1 - 97, stage 2 - 113) undergoing low dose CT for lung cancer screening purposes and 99 consecutive COPD patients (GOLD stage 3 - 48, stage 4 - 51) undergoing CT scan in a stable condition for clinical evaluation of COPD were included. Fully automated lobar emphysema quantification was performed using "MeVis PULMO 3D" tool (MeVis Research, Bremen, Germany). The ratio of emphysema index in the upper lobes (upper and middle right + upper left) to emphysema index in the lower lobes was calculated in each subject.

Results: In lower GOLD stages (at risk, 1 and 2) represented in the screening cohort a broad range (0.3 -14, median 2.27, interquartile range 1.4 - 4.1) of ratios with a clear predominance of - beginning - emphysema in the upper lobes was found. In severe GOLD stages (3 and 4), represented in the clinical cohort, the ratios had a far lower range and scattered around 1 (range 0.3 - 6.4, median 1.1, interquartile range 0.9 - 1.4), implicating far more homogeneous emphysema distribution between upper and lower lobes.

Conclusion: In our study cohort emphysema distribution between upper and lower lobes differed significantly in early and late COPD stages. Measuring emphysema inhomogeneity is thought to bring new aspects to phenotyping COPD and further understanding of the development of this complex disorder.

P40

Diffusion weighted MR imaging vs. FDG-PET/CT: Predictive capabilities of therapeutic effect and survival in non-small cell lung cancer patients before chemoradiotherapy

Ohno Y.¹, Nishio M.¹, Koyama H.¹, Onishi Y.¹, Matsumoto K.^{1,2}, Takenaka D.¹, Matsumoto S.¹, Yoshikawa T.¹, Sugimura K.¹

¹Kobe University Graduate School of Medicine, Radiology, Kobe, Japan, ²Yamanashi University, Radiology, Chuo, Japan

Purpose: To compare the predictive capabilities of diffusion-weighted MR imaging (DWI) and FDG-PET/CT for therapeutic effect and survival in non-small cell lung cancer (NSCLC) patients before chemoradiotherapy.

Materials and methods: Sixty-four NSCLC patients (38 men and 26 women; age range 56-78 years), diagnosed as stage III, who underwent pre-therapeutic DWI and FDG-PET/CT and were treated with chemoradiotherapy. For quantitative prediction, apparent diffusion coefficient (ADC) for DWI and maximum standard uptake value (SUV_{max}) for PET/CT were measured at all targeted lesions and averaged to obtain final values for each subject. To evaluate the predictive capability of either index for distinguishing partial response and non-response (stable or progressive disease) groups, ROC analysis was performed, while sensitivity, specificity and accuracy of the two modalities were compared



by using McNemar's test. Finally, overall and progression-free survival (OS and PFS) curves divided by the corresponding threshold value were compared by means of log-rank test.

Results: Area under the curve (Az) for ADC (Az = 0.84) was significantly larger than that for SUV_{max} (Az=0.64, p< 0.05). The application of feasible threshold values resulted in specificity (44.4 %) and accuracy (76.6 %) of DWI becoming significantly higher than those of PET/CT (specificity: 11.1 %, p< 0.05; accuracy: 67.2 %, p< 0.05). In addition, only OS and PFS of the two groups divided by the threshold value for ADC showed significant difference (p< 0.05).

Conclusion: DWI may have better potential than FDG-PET/CT for prediction of therapeutic effect and survival in NSCLC patients before chemoradiotherapy.

P41

4D magnetic resonance velocity mapping of blood flow patterns in the pulmonary outflow tract (RVOT) and proximal main pulmonary artery (PA) after Shelhigh porcine graft reconstruction

Poschenrieder E.¹, Fellner C.¹, Buchner S.², Debl K.², Kobuch R.³, Pühler T.³, Dornia C.¹, Stroszczyński C.¹, Hamer O.W.¹

¹University Medical Center of Regensburg, Radiology, Regensburg, Germany,

²University Medical Center of Regensburg, Cardiology, Regensburg, Germany,

³University Medical Center of Regensburg, Cardiac Surgery, Regensburg, Germany

Purpose: Patients with a Shelhigh pulmonic porcine graft reconstruction of the right ventricular outflow tract (RVOT) related to Ross procedure frequently show hemodynamically relevant postoperative pulmonary stenosis. The aim of this study was to evaluate if color-coded visualization and quantification of time-resolved 3D phase contrast (PC) MRA data ("4D Flow") is clinically viable to determine distorted blood flow patterns after Shelhigh reconstruction.

Materials and methods: Nine symptomatic patients with a Shelhigh reconstruction underwent oblique sagittal 4D Flow of the RVOT and proximal pulmonary artery (PA) at 1.5T. A dedicated postprocessing software was used to qualitatively and quantitatively analyze flow patterns. Maximum velocity data were correlated with conventional 2D PC MRA data.

Results: Six patients showed mild, 2 patients moderate and 1 patient severe stenosis of the RVOT/PA, with various degrees of flow distortion and acceleration in the RVOT/PA. 4D Flow was technically successful with demonstrative visualization of flow patterns in all cases. Maximum velocities in the RVOT/PA were up to 232 cm/s in cases of mild, up to 279 cm/s in cases of moderate, and 320 cm/s in case of severe stenosis. Discrepancies between 2D PC MRA and 4D Flow velocities were found to be due to slice positioning of 4D Flow not in plane of peak velocity.

Conclusions: 4D Flow is an easy and fast method for qualitative and quantitative assessment of complex blood flow patterns in the reconstructed RVOT/PA in patients

who underwent a Ross procedure. Discrepancies to 2D data were due to slice positioning.

P42

Screening for interstitial lung disease in systemic sclerosis: Diagnostic accuracy of hrct image series with high increment and reduced number of slices

Winklehner A.¹, Berger N.¹, Distler O.², Alkadhi H.¹, Frauenfelder T.¹

¹University Hospital of Zurich, Institute of Diagnostic Radiology, Zurich, Switzerland,

²University Hospital of Zurich, Department of Rheumatology, Zurich, Switzerland

Purpose: To assess diagnostic accuracy for detection of interstitial lung disease (ILD) in different image series with high increment and reduced number of slices compared to the standard high-resolution CT (HRCT) in patients with known systemic sclerosis (SSc).

Material/Methods: 45 consecutive patients (38 female; mean age 57.9±13.9 years) with known SSc underwent HRCT. Three series of secondary captures were reconstructed as following: 1) series with 10 mm increment and 1mm slices, 2) series of three axial images obtained apical, at the level of the carina and basal, 3) series of seven axial images with baso-apical gradient. Two blinded radiologists independently recorded presence of ILD, degree of diagnostic confidence, and HRCT pattern. Furthermore, the effective dose for each image series was estimated. Standard HRCT was Standard of Reference.

Results: Prevalence of ILD was 55% (n=25). Sensitivity of all image series in detecting IDL was high, ranging from 100% in series 1, to 92-96%, and 88-96% in series 3 and 2, respectively. Accuracy ranged from 93.3-95.5% for image series 2 and 3, to 97.8% for image series 1. Estimated dose reduction was 90.5% for series 1 (0.154 mSv; standard of reference 1.624 mSv) and more than 98% for series 2 and 3 (0.014 mSv; 0.028 mSv).

Conclusion: HRCT image series with high increment and reduced number of slices allow an accurate detection of ILD with very low radiation dose, making this approach valuable for screening.

P43

Diffuse Pulmonary Ossification (DPO): CT findings

Gruden J.F.¹, Panse P.M.¹, Trahan A.M.¹

¹Mayo Clinic Arizona, Radiology, Phoenix, United States

Purpose: We characterize the CT features of diffuse pulmonary ossification (DPO) in patients with and without visible features of interstitial fibrosis.

Methods: We performed a retrospective computerized search of radiology reports between 2000-2010 at our institution for the word "ossification" and identified 23 unique patients. CT examinations were reviewed by 2 readers and findings reported by consensus.

Results: Findings of interstitial fibrosis were present in 16 and absent in 7 patients.



Areas of characteristic high density were present in the interlobular septae and subpleural and subfissural spaces (pulmonary interstitium) with a lower zone predominance in all instances.

Conclusions: DPO has a characteristic CT appearance. DPO is known to occur in some patients with fibrosis, particularly usual interstitial pneumonitis (UIP), but it can also occur as an independent finding in the absence of fibrosis. The cause is not known, but the presence of DPO in isolation is not diagnostic of UIP.

P44

Poster withdrawn

P45

MDCT in detection of Hantavirus lung forms

Ivkovic A.T.¹, Milosavljevic T.T.²

¹Clinical Center Nis, Center of Radiology, Nis, Serbia, ²ZC Vranje, Radiology, Nis, Serbia
Hantaviruses belong to the Bunyaviridae family of viruses. Lung forms are rare.

Aim of the study: The main aim is to show cases of Hantavirus pneumonia in child population.

Material and methods: We examined 64 patients with confirmed Hantavirus pneumonia. The youngest patient was 4 years old, the oldest 84. We examined all patients on 16 or 64 MDCT.

Results: After the major flood we had few outbreaks, one of them was Hantavirus with mainly pulmonary form. All patients were from rural parts with no medical institution near, so patients went to medical care in late phase of illness. In the first phase symptoms were similar or same as influenza like fever, chills, sweaty palms, diarrhea, malaise, headaches, nausea, abdominal and back pain, tachycardia and hypoxemia but in the late phase occur a lot of different symptoms. CT signs develop rapidly and constantly, first one sided mostly near hilum but as time goes by illness went to other side. First radiology sign is similar to bronchiolitis and after that massive inflammation, than again bronchiolitis in next lung segment. In the lethal cases (28, 33.33%) illness develop for two months, each day symptoms were worse. We had 3 patients with massive hemoptysis and bleeding after hemodialysis.

Conclusion: Lung form of Hantavirus illness is very often lethal. Understanding the way of developing can be vital for patient life. CT is powerful tool for diagnostic.

P46

Comparison of the effect of intravenous low-osmolal iopamidol and iso-osmolal iodixanol on heart rate during non-gated chest CT angiography - Results of a prospective randomized multicentric study

Chartrand-Lefebvre C.¹, White C.², Prenovault J.³, Bhalla S.⁴, Mayo-Smith W.⁵, Vydareny

K.⁶, Soto J.⁷, Ozkan O.⁸, Chughtai A.⁹, Gorgos A.³, Soulez G.³

¹University of Montreal Medical Center (CHUM), Hôtel-Dieu hospital, Radiology, Montreal, Canada, ²University of Maryland Hospital, Baltimore, United States, ³University of Montreal Medical Center (CHUM), Radiology, Montreal, Canada, ⁴Mallinckrodt Institute of Radiology, St. Louis, United States, ⁵Rhode Island Hospital, Providence, United States, ⁶Emory University, Atlanta, United States, ⁷Boston Medical Center, Boston, United States, ⁸University of Texas, Galveston, United States, ⁹University of Michigan, Ann Arbor, United States

Purpose: To compare the effect on heart rate (HR) of intravenous (IV) injection of low-osmolal iopamidol and iso-osmolal iodixanol during non-gated chest CT angiography (CTA).

Method/Materials: Prospective, multicenter, double-blind, randomized, parallel-group study comparing iopamidol-370 and iodixanol-320 (8 centers). 130 consecutive patients (54M, mean age 52) with suspicion of pulmonary embolism referred for pulmonary CTA were included. 63 patients received iopamidol and 67 patients received iodixanol (80 ml IV, 4ml/s). 64-slice MDCT was used on the entire chest (breath-hold, end-inspiration). No patients received prescan beta-blocker. Precontrast HR (bpm) was obtained \leq 5 minutes before injection and HR was monitored from start of injection to end of scanning, for maximum HR recording. Unpaired t test and χ^2 were used for continuous and categorical variables, respectively.

Results: Precontrast HR was similar in both groups (iopamidol: mean 81 ± 17 bpm; iodixanol: mean 76 ± 17) ($p=0.16$). HR showed a slight increase in both groups after contrast administration. Mean change from precontrast to maximum postcontrast HR was 5.4 ± 8.8 for iopamidol and 5.4 ± 7.3 for iodixanol. The difference between the two groups was not statistically significant ($p=0.72$). Near half of the patients in each group showed an increase < 5 bpm (iopamidol: 35 patients, 55.6%; iodixanol: 33 patients, 49.3%).

Conclusion: High rate IV administration of iopamidol and iodixanol during pulmonary CTA slightly increased HR, with no difference in HR changes between the two agents. Since HR control is critical during ECG-gated CT, these results suggest that either agent is suitable for use in cardiac or other ECG-gated CT studies.

P47

Pandemic influenza A (H1N1) 2009: Chest imaging findings from 147 proven cases in a university hospital

Semionov A.¹, Tremblay C.², Samson L.¹, Chandonnet M.¹, Chalaoui J.³, Chartrand-Lefebvre C.¹

¹University of Montreal Medical Center (CHUM), Hôtel-Dieu hospital, Radiology, Montreal, Canada, ²University of Montreal Medical Center (CHUM), Hôtel-Dieu hospital, Microbiology, Montreal, Canada, ³University of Montreal Medical Center (CHUM), Radiology, Montreal, Canada



Purpose: To describe the radiographic features and prognostic imaging findings in patients with isolated and complicated acute infection by the novel influenza A (H1N1) virus.

Method/Materials: Retrospective study of 147 patients (64 M, mean age 41) with confirmed real-time reverse transcriptase polymerase chain reaction acute influenza A (H1N1) infection, who also had a chest radiograph within 72 hours of the collection of viral specimen. Radiographs and CT scans were analyzed for acute findings. Correlation with bacterial culture results was performed. Unpaired student t-test and Pearson χ^2 test were used, respectively for continuous and discrete variables.

Results: In 71% of cases, chest radiograph was normal. Presence of acute imaging findings was associated with older age ($p < 0.05$), increased rate of comorbidities (chronic obstructive pulmonary disease, diabetes, asthma) ($p < 0.05$), higher incidence of hospitalization ($p < 0.05$) and ICU admission, and increased mortality. Predominant radiographic findings in isolated primary influenza A (H1N1) were alveolar opacities (88%), either unifocal or multifocal, preferentially in the lower lobes; and ground-glass opacities on CT (100%). In the subgroup of patients with positive imaging findings and available bacterial microbiological data, 62% suffered superimposed bacterial infection.

Conclusion: In acute influenza A (H1N1) infection, the chest radiograph is most often normal. Imaging findings are associated with older age, increased rate of comorbidities, and hospitalization, and consist of alveolar opacities on radiography, and ground-glass opacities on CT. Superimposed bacterial infection is frequent, and must be excluded in patients with abnormal imaging.

P48

Aortic extension of catheter-induced coronary artery dissection: Diagnosis, grading and follow-up with MDCT

Tanasie C.¹, Chandonnet M.^{1,2}, Chin A.^{1,2}, Kokis A.³, Perrault L.L.⁴, Ly H.⁵, Doucet S.⁵, Gorgos A.⁶, Chartrand-Lefebvre C.^{1,2}

¹University of Montreal Medical Center (CHUM), Hôtel-Dieu hospital, Radiology, Montreal, Canada, ²Montreal Heart Institute, Radiology, Montreal, Canada, ³University of Montreal Medical Center (CHUM), Hôtel-Dieu hospital, Cardiology, Montreal, Canada, ⁴Montreal Heart Institute, Surgery, Montreal, Canada, ⁵Montreal Heart Institute, Cardiology, Montreal, Canada, ⁶University of Montreal Medical Center (CHUM), Radiology, Montreal, Canada

Purpose: To describe the MDCT (multidetector CT) imaging findings, grading and evolution of retrograde aortic extension of catheter-induced coronary artery dissection, an infrequent complication of cardiac catheterization.

Methods and Materials: Retrospective analysis of the MDCT imaging data and follow-up of 8 cases of catheter-induced aortocoronary dissection. A grading classification of the aortocoronary dissection according to the superior aortic extension is proposed.

Results: Catheter-induced aortocoronary dissection involved the right coronary artery in

seven patients (88%), and the left coronary artery in one patient. Coronary artery stenting was successful in seven cases. One stenting failure required surgery, with subsequent death.

Unenhanced MDCT showed the high attenuation material in the aortic wall, caused by the residual contrast agent used during catheter angiography, and MDCT angiography allowed direct visualization of the false and true lumen. There were three cases of grade 1, three cases of grade 2 and two cases of grade 3 aortocoronary dissection. Follow-up imaging with MDCT in all clinically stable patients demonstrated a gradual decrease in the length and diameter of the iatrogenic aortic dissection (48 h to 6 weeks).

Conclusion: Catheter-induced aortocoronary dissection is usually treated with immediate coronary artery stenting of the entry point. Subsequent non invasive imaging for further evaluation, grading and close monitoring of the aortic retrograde extension of the dissection can be safely done with MDCT.

P49

Methicillin-resistant *Staphylococcus aureus* and methicillin-susceptible *Staphylococcus aureus* pneumonia: Comparison of clinical and thin-section CT findings

Okada F.¹, Ando Y.², Morikawa K.¹, Ono A.¹, Matsushita S.¹, Ishii R.¹, Mori H.¹

¹Oita University Faculty of Medicine, Radiology, Yufu, Japan, ²Nishibeppu National Hospital, Radiology, Beppu, Japan

Purpose: The aim of this study was to compare the clinical and thin-section CT findings in patients with methicillin-resistant *Staphylococcus aureus* (MRSA) and methicillin-susceptible *Staphylococcus aureus* (MSSA).

Materials and methods: We retrospectively identified 201 patients with acute MRSA pneumonia and 164 patients with acute MSSA pneumonia who underwent chest thin-section CT examinations between January 2004 and March 2009. Patients with concurrent infectious disease were excluded from our study. Consequently, our study group comprised 68 patients with MRSA pneumonia (37 male, 31 female) and 83 patients with MSSA pneumonia (32 male, 51 female). Clinical findings in the patients were assessed. Parenchymal abnormalities, lymph node enlargement, and pleural effusion were assessed.

Results: Underlying diseases such as cardiovascular were significantly more frequent in the patients with MRSA pneumonia than in those with MSSA pneumonia. CT findings of centrilobular nodules, especially with a tree-in-bud pattern, and bronchial wall thickening were significantly more frequent in the patients with MSSA pneumonia than those with MRSA pneumonia ($p=0.038$, $p=0.007$, and $p=0.039$, respectively). In the group with MRSA, parenchymal abnormalities were observed to be mainly peripherally distributed and the frequency was significantly higher than in the MSSA group ($p=0.028$). Pleural effusion was significantly more frequent in the patients with MRSA pneumonia than those with MSSA pneumonia ($p=0.002$).



Conclusions: Findings from the evaluation of thin-section CT manifestations of pneumonia may be useful to distinguish between patients with acute MRSA pneumonia and those with MSSA pneumonia.

P50

Thin-section computed tomography findings of patients with acute *Streptococcus pneumoniae* pneumonia with and without concurrent infection

Ando Y.¹, Okada F.², Matsushita S.², Ishii R.², Nakayama T.², Morikawa K.², Mori H.²

¹Nishibeppu National Hospital, Radiology, Oita, Japan, ²Oita University Faculty of Medicine, Oita, Japan

Purpose: To compare the pulmonary thin-section computed tomography (CT) findings of patients with acute *Streptococcus pneumoniae* pneumonia with and without concurrent infection.

Materials and methods: The study group comprised 86 patients with acute *S. pneumoniae* pneumonia, 36 patients with *S. pneumoniae* pneumonia combined with *Haemophilus influenzae* infection, 26 patients with *S. pneumoniae* pneumonia combined with *Pseudomonas aeruginosa* infection, and 22 patients with *S. pneumoniae* pneumonia combined with methicillin-susceptible *Staphylococcus aureus* (MSSA) infection.

We compared the clinical and thin-section CT findings among the groups.

Results: Underlying health issues, such as smoking and malignancy, were significantly more frequent in patients with pneumonia caused by concurrent infection than those infected with *S. pneumoniae* alone. Centrilobular nodules and bronchial wall thickening were also significantly more frequent in patients with pneumonia caused by concurrent infection (*H. influenzae*: $p < 0.001$ and $p < 0.001$, *P. aeruginosa*: $p < 0.001$ and $p < 0.001$, MSSA: $p < 0.001$ and $p < 0.001$, respectively) than in those infected with *S. pneumoniae* alone. Cavity and bilateral pleural effusions were significantly more frequent in cases of *S. pneumoniae* pneumonia with concurrent *P. aeruginosa* infection than in cases of *S. pneumoniae* pneumonia alone ($p < 0.001$ and $p < 0.001$, respectively) or with concurrent *H. influenzae* ($p < 0.05$ and $p < 0.001$, respectively) or MSSA infection ($p < 0.05$ and $p < 0.05$, respectively).

Conclusion: When a patient with *S. pneumoniae* pneumonia has centrilobular nodules and bronchial wall thickening on CT images, concurrent infection should be considered.

P51

Synchronous persistent Eustachian valve and atrial septal aneurysm mimicking atrial septal defect on echocardiogram

Egger L.¹, Husser O.², Endemann D.², Hamer O.W.¹

¹University Medical Center of Regensburg, Institut of Radiology, Regensburg, Germany,

²University Medical Center of Regensburg, Dept. of Internal Medicine II, Regensburg, Germany

Purpose: We report the case of a woman whose echocardiographic findings were suspicious for an atrial septal defect.

Material and Methods/Results: A transoesophageal echocardiogram in a 48 year old woman revealed an atrial septal aneurysm and was suspicious for an ostium secundum defect. For further evaluation a cardiac MRI was performed. A membranous structure was seen that originated from the ostium of the inferior vena cava and protruded upwards into the right atrium. The bulging right atrial septum gained close proximity to this membrane. Due to its typical location the membrane was diagnosed to be a prominent persistent Eustachian Valve. A defect of the atrial septum was excluded because there was no detectable jet and a left-to-right shunt was ruled out by phase contrast imaging. Repeat review of the echocardiogram revealed that the jet through the small canal between the bulging septum and the Eustachian valve had mimicked a transseptal jet.

Conclusion: To the best of our knowledge this is the first case in literature with MRI visualization of a synchronous persistent Eustachian valve and an atrial septal aneurysm. The case emphasizes that cardiac MRI is an excellent tool for depiction of the anatomy of the heart and is superior to echocardiogram in the presence of anatomic variants.

P52

Subpleural micronodular pattern at CT and radiopathologic correlation.

Cabrera G.¹, Roma de Villegas E.¹, Domingo Montañana M.L.¹, Fernandez Ruiz C.P.¹, Cortés Vizcaino V.², Vilar Samper J.L.¹

¹University Hospital Dr. Peset, Department of Radiology, Valencia, Spain,

²University Hospital Dr. Peset, Department of Pathology, Valencia, Spain

Purpose: To review all thoracic diseases which may associate subpleural parenchymal micronodules; to describe and classify these subpleural and perifissural small nodules according to their differential CT imaging features and show their pathologic correlation.

Material/Methods: We retrospectively reviewed all standard and thin-section chest CT scans made in our Radiology department from January 2006 to January 2011 and evaluated those with a positive report for subpleural micronodules. A correlation between radiologic (through CT) and histopathologic findings was made when both studies were available.

Results: Subpleural micronodules (SBM) are defined as rounded parenchymal lesions up to 7 mm of diameter observed beneath the pleura. They are a common sign in certain interstitial lung diseases such as sarcoidosis, coal's worker's pneumoconiosis or lymphangitic carcinomatosis; SBM may be also present in follicular bronchiolitis or appear isolated in healthy smokers (and related to anthracosis), making necessary a correct differential diagnosis with intraparenchymal lymph nodes. Classification should be made according to their lung distribution, number of lesions or presence of calcification.

Conclusion: Subpleural micronodules represent a frequent incidental and isolated finding specially in patients with a smoking history. However, when associated with additional pulmonary findings, they may facilitate the appropriate diagnosis of diverse diffuse infiltrative lung diseases.



P53

Advanced CT methods in detection of rare lung diseases

Milosavljevic T.¹, Ivkovic A.²

¹ZC Vranje, Radiology, Vranje, Serbia, ²Clinical Center Nis, Center of Radiology, Nis, Serbia

Purpose: Is to determine ways of detecting of rare lung pneumonias and to find a most appropriate tool for differential diagnosis of lung inflammation.

Material and methods: We examined 4778 patients with pneumonia. From that number 4601 were with common pneumonias. Rest of them (177) was with rare forms of pneumonia. We perform standard 64 MDCT, 64 HRMDCT, 3D virtual bronchoscopy, 3D nodule check and 64MDCT pulmonary angiography. Patients were from 4 year old (Hanta virus) to 87 (parasitic pneumonia). Male were 97, female 80 patients.

Results: We divide results by type of infection; by each CT examine results and by final prognosis for the patient. By type we divide in bacterial (Chlamydomphila pneumoniae, Mycoplasma pneumoniae, Legionella pneumophila Klebsiella pneumoniae, Escherichia coli, Pseudomonas aeruginosa, Moraxella catarrhalis etc.), viral (Hanta etc.), fungal (Cryptococcus neoformans, Pneumocystis jiroveci, and Coccidioides immitis), parasite (Toxoplasma) and other types (desquamative interstitial pneumonia). By CT we divide in main radiology signs like side, territory, existence of bronchiolitis, necrosis etc. Our main interest was in differences in 3D analysis and in CT angiography. For each cause of pneumonia we track results and try to find most often and most specific signs to determine differences and find exact diagnosis. All methods together bring enough information to make exact diagnosis. Very important was tracking the progress and speed of development. Also prognosis of patients was track.

Conclusion: Combination of different methods gives excellent results in finding the right diagnosis

P54

CT in lung injuries caused by fire

Milosavljevic T.¹, Ivkovic A.²

¹ZC Vranje, Radiology, Vranje, Serbia, ²Clinical Center Nis, Center of Radiology, Nis, Serbia

Lungs in fire accidents can be injured by hot air, smoke or by chemical agents. Fire accidents are very often. Symptoms after injury can be acute or late.

Purpose: Main purpose is to show effects of fire on the lung and to show radiological signs of lung injuries.

Methods: We 173 patients fire. All patients were examined on 16 or 64 MDCT. Male patients were 91, female 82. The youngest patient was 4 years old; the oldest was 84 years old. We perform standard MDCT examination followed by virtual bronchoscopy. We examined 101 patients with acute symptoms and 72 with symptoms 24 to 48 hours after accident.

Results: We separate radiological findings in 3 groups according to cause of injury. First group were patients with hot air as cause of lung injury. In this group there were 41 patients, all in acute form. Main injuries were on upper respiratory system. Second group were patients with smoke as injury cause. In this group we examined 109 patients. Patients were with different clinical and radiological signs, mostly with signs of pneumonia. Third group were patients after inhalation of different chemical agents. In this group we examined 23 patients. Almost all of them had serious alveolar injuries. There were 11 patients finished lethally. 76 other patents were with serious health damages.

Conclusion: Fire brings a lot of serious lung injuries. CT is the main diagnostic tool for detection.

P55

Poster withdrawn

P56

In vivo micro-CT in various mouse asthma models: integrated assessment of airway inflammation and remodelling

Lederlin M.¹, Dournes G.¹, Ozier A.², Montaudon M.¹, Berger P.², Laurent F.¹

¹CHU Bordeaux, Imagerie Medicale, Pessac, France, ²CHU Bordeaux, Physiologie Respiratoire, Pessac, France

Purpose: To determine whether in-vivo micro-CT is able to demonstrate airway inflammation and remodelling in a mouse asthma model.

Material and method: Thirty BALB/C mice were challenged intranasally with ovalbumin. Three endpoints were used to obtain three histological patterns of allergic asthma: inflammation, inflammation and remodelling, and remodelling. Thirty other mice were challenged with saline to constitute control groups. All mice underwent plethysmography and micro-CT. The mice were then sacrificed and lungs examined histologically. From the micro-CT images, the total lung attenuation (TLA) and peribronchial attenuation (PBA) were semi-automatically extracted. A semi-automatic method for PBA extraction was assessed against a method of reference. Plethysmographic, micro-CT, and histological data were compared between asthmatic and control mice. Correlations were assessed between micro-CT bronchial parameters, *i.e.* PBA and 1-PBA/TLA, and plethysmographic and histological data.

Results: Fifty-one mice completed the study. The asthmatic mice fulfilled the histological criteria for each asthmatic pattern. The semi-automatic method for PBA measurement showed a good agreement with the method of reference. PBA was significantly different in mice exhibiting inflammation and remodelling ($P < 0.001$). 1-PBA/TLA was significantly different in mice exhibiting inflammation and remodelling ($P < 0.001$), and remodelling only ($P = 0.01$). PBA correlated better than 1-PBA/TLA with inflammation. 1-PBA/TLA correlated with remodelling especially with bronchial smooth muscle and fibrosis.



Conclusion: In vivo respiratory-gated micro-CT allows a non-invasive integrated assessment of airway inflammation and remodelling. 1-PBA/TLA appears to be a reliable biomarker of remodelling. This should be considered for the use of micro-CT in monitoring new drugs targeting bronchial remodelling.

P57

Idiopathic interstitial pneumonias: UIP vs Not-UIP

Coelho M.L.O.D.O.¹, Fonseca M.A.², Maciel J.³, Santiago I.³, Saraiva A.³, Reis D.³, Castaño J.²

¹Hospital Infante d Pedro, Radiologia, Aveiro, Portugal, ²Hospital Pulido Valente, Lisboa, Portugal, ³Hospital Infante d Pedro, Aveiro, Portugal

Learning objectives: Review HRCT and anatomo-pathologic findings that distinguish UIP from other idiopathic interstitial pneumonias.

Background: The idiopathic interstitial pneumonias (IIPs) are a collection of diseases of unknown etiology usually associated with the presence of various degrees of fibrosis and inflammation. The classification of idiopathic interstitial pneumonias is based on histologic criteria, giving rise to seven morphologic patterns, which correlate to imaging patterns on high-resolution computed tomography. Each of them - usual interstitial pneumonia (UIP), nonspecific interstitial pneumonia (NSIP), desquamative interstitial pneumonia (DIP), respiratory bronchiolitis interstitial lung disease (RB-ILD), acute interstitial pneumonia (AIP), cryptogenic organizing pneumonia (COP), and lymphoid interstitial pneumonia (LIP) - is described as having typical histopathologic and imaging characteristics. However, in practice, the clinical features, the imaging patterns and even the histologic findings may be variable and overlapping, what, associated with significant differences in prognosis and accuracy levels of HRCT diagnosis, has led that idiopathic interstitial pneumonias are classified broadly as: usual interstitial pneumonia (UIP) and idiopathic interstitial pneumonias other than usual interstitial pneumonia (Not-UIP).

Imaging findings/Procedure details: Single slice CT and 16 multidetector CT acquired exams were compared with its corresponding histopathology. We review not only the typical radiological characteristics that distinguish idiopathic interstitial pneumonia, but also the confounding aspects that had given rise to less accurate diagnosis.

Conclusion: The first step of radiological distinction of UIP vs not-UIP gives rise to a subsequent multidisciplinary approach and defines the need of surgical lung biopsy.

P58

Incidence and causal factors of inadequate interpretation of chest radiography in patients with lung cancer

Gil Gallego J.C.¹, Pallarés Sanmartín A.², Tilve Gómez A.¹, Rodríguez Fernández P.¹, Cea Pereira S.¹, Represas Represas C.³, García-Tejedor J.L.¹, Fernández Villar A.³

¹Complejo Hospitalario Universitario de Vigo, Radiology, Vigo, Spain, ²Complejo

Hospitalario de Pontevedra, Respiratory Medicine, Pontevedra, Spain, ³Complejo Hospitalario Universitario de Vigo, Respiratory Medicine, Vigo, Spain

Purpose: This study was carried out to detect the previous pathological chest radiography (CR) in subjects with lung cancer (LC) in our center and the reasons because they went unnoticed.

Materials and methods: We did a retrospective cohorts study in which we included all patients with a confirmed diagnosis of LC in our center between January 2007 and November 2008. Cases that had a CR two years before the suspected diagnosis were chosen and they were individually analyzed by a thoracic radiologist and an expert chest physician.

Results: 185 patients were diagnosed with LC in our center in that period, of whose we could review 59 patients with a previous CR (32%). From these patients 43 had a pathological previous CR (23%), more than 73% of the cases lesions are bigger than 1 cm. The average delay in the diagnosis was 308.6 days (± 183.5).

The principal factors of the inadequate interpretation of CR were the hilar or mediastinal location (34%), the overlap with bone structures (18,7%) and the absence of a follow-up of the lesions (5,1%); however this inadequate interpretation does not influence the rate of advanced stages.

Kappa index of agreement between the CR report of radiologist and chest physician was 0,73.

Conclusions: 23% of the patients diagnosed with LC presented a pathological CR two years before.

Hilar location and the overlap with bone structures are the main causes of misdiagnosis. These results did not suppose a higher incidence of advanced stages in these patients.

P59

A comparative evaluation of CT-based automated lobar emphysema quantification, manually corrected method, and visual assessment at different clinical stages

Koyama H.¹, Owsijewitsch M.², Ley S.², Puderbach M.³, Heussel C.P.⁴, Herth F.J.F.⁵, Kuhnigk J.-M.⁶, Kauczor H.-U.²

¹Kobe University School of Medicine, Radiology, Kobe, Japan, ²Heidelberg University, Diagnostic and Interventional Radiology, Heidelberg, Germany, ³German Cancer Research Center, Radiology, Heidelberg, Germany, ⁴Thoraxklinik Heidelberg, Interventional and Diagnostic Radiology with Nuclear Medicine, Heidelberg, Germany, ⁵Thoraxklinik Heidelberg, Pneumology, Heidelberg, Germany, ⁶Fraunhofer MEVIS - Institute for Medical Image Computing, Bremen, Germany

Purpose: To compare automated lobar emphysema quantification (LEQ) with a manually corrected method and visual assessment.

Material/Methods: Non-enhanced thin-section CT-data of the chest were consecutively



selected from patients suffering from pulmonary emphysema (N = 129, 87 men and 42 women; mean age 61.0 years). They were classified by disease stage into five groups based on the Global Initiative for Chronic Obstructive Lung Disease (GOLD) classifications (stage 0 [n =34], stage 1 [n =22], stage 2 [n = 35], stage 3 [n =21], and stage 4 [n =17]). Low-attenuation volume proportions (emphysema index, EI) of each lobar parenchyma were measured in a fully automated and a manually corrected mode, and visual assessment was performed. These results of the three methodologies were compared as well as agreement in lobar predominance detection was analyzed statistically.

Results: EI of automated and manual LEQ were not significantly different (paired t test, $p > 0.05$) and had excellent correlation ($r > 0.94$, $p < 0.0001$), both overall and within each stage of COPD. The EI from automated LEQ correlated moderately well with visual scores, both overall and at each stage ($0.63 < r < 0.80$, $p < 0.001$). Agreement between automated and manual LEQ in lobar predominance detection at all stages was either substantial or almost perfect ($\kappa > 0.70$). Agreement between automated LEQ and visual assessment at stages 3 and 4 was substantial ($\kappa > 0.63$).

Conclusion: Automated lobar emphysema quantifications showed good agreement with both manually corrected method and visual assessment.

P60

A novel optical navigation system for CT-guided fine needle aspiration biopsies of small (≤ 15 mm) pulmonary lesions

Aviram G.¹, Schwarz Y.², Man A.², Tiran B.², Mercer D.¹, Rosen Tirosh G.¹, Sosna J.³

¹Tel-Aviv Medical Center, Radiology, Tel-Aviv, Israel, ²Tel-Aviv Medical Center, Pulmonology, Tel-Aviv, Israel, ³Hadassah Hebrew University Medical Center, Radiology, Jerusalem, Israel

Purpose: To prospectively evaluate the safety and accuracy of a novel optical navigation system in CT guided aspiration biopsies of small pulmonary lesions.

Method and materials: The study was performed with IRB approval and patients' informed-consent. It included 24 consecutive patients, with pulmonary lesions ≤ 15 mm suspected of malignancy. CT guided fine needle aspirations (FNA) using ActiSight Needle Guidance System (ActiViews Ltd. Haifa Israel), were done with 20G Chiba needles. The system consists of a pad with fiducial markers, and a miniature video camera mounted on the biopsy needle and provides real-time needle guidance information.

Accuracy of reaching the center of the target lesions, procedure time, number of needle passes through the pleura, number of CT scans during needle advancement and rate of complications were recorded.

Results: Patients were 42-84 (mean 68) years, lesion diameter 6.7-15mm (11.4 ± 2.9 mm), distance from skin to lesion 47-116mm (71.2 ± 17.3 mm). Lesions have been successfully reached in 23/24 (96 %), with distance from needle tip to lesion center of 2.8 ± 2.2 mm. One case required 2 needle passes. FNA samples were evaluated as adequate for diagnosis by on-site cytology in 19/24 (79%) of the cases, malignancy found in 53%. Mean number of CT scans during needle advancement was 2.9 ± 2.1 (0-7). Mean

procedure time was 31 ± 10 min. Small post procedural pneumothoraces were detected in 4/24 (17%) of the cases; none required chest tube placements or hospitalization.

Conclusion: Our results suggest that the use of this novel needle guidance system in biopsies of small pulmonary lesions is safe and accurate.

P61

The role of CAD in the detection of low conspicuity nodules on chest radiographs

Shaham D.¹, Issac L.^{2,3}, Bogot N.R.⁴, Manevitch A.², Lederman R.¹

¹Hadassah-Hebrew University Medical Center, Department of Radiology, Jerusalem, Israel, ²Siemens Computer Aided Diagnosis, Jerusalem, Israel, ³Jerusalem College of Technology, Department of Medical Engineering, Jerusalem, Israel, ⁴Shaarei Zedek Medical Center, Department of Radiology, Jerusalem, Israel

Purpose: To evaluate the ability of CAD to detect on chest radiographs, low conspicuity lesions of various consistencies.

Material and methods: 108 digital frontal chest-radiographs were retrospectively correlated to CT by 2 independent expert readers who identified on the radiographs 154 lung nodules, and assigned them conspicuity (1-low or 2- high) and consistency scores. The 110 solid lesions were subdivided into smooth, lobular and irregular. The other 44 lesions were subdivided into cavitory, sub-solid and indeterminate. All radiographs were run with a prototype CAD algorithm (Siemens) to determine performance by lesion consistency and conspicuity. CAD prompts not corresponding to CT-verified findings were considered false.

Results: The overall CAD sensitivity was 79.9%, with a false-mark rate of 1.9. The CAD sensitivity for non-solid nodules (81.8%) was similar ($p=0.44$) to that of solid nodules (79.1%), although their conspicuity was significantly ($p < 0.001$) lower (1.07 vs. 1.57). Conspicuity, whether low or high, did not affect the CAD sensitivity for either solid nodules (78.7% vs. 79.4%, $p=0.47$) or non-solid nodules (80.8% vs. 83.3%, $p=0.42$). Although the mean conspicuity of solid lobular nodules (1.79) was significantly higher ($p < 0.03$) than of smooth nodules (1.51), the CAD sensitivity was not significantly affected (89.5% vs. 79.6%, $p=0.29$). The CAD sensitivity of indeterminate opacities (88.5%) was similar ($p=0.47$) to that of part-solid nodules (87.5%), although their conspicuity was significantly higher (1.42 vs. 1.13, $p < 0.04$).

Conclusion: CAD performance on chest radiographs was independent of both nodule consistency and conspicuity. Thus, CAD should be useful for less conspicuous nodules.

P62

New denoising technique on low-dose CT: Usefulness for quantification of pulmonary emphysema

Nishio M.¹, Matsumoto S.¹, Ohno Y.¹, Sugihara N.², Yoshikawa T.¹, Takenaka D.¹,



Sugimura K.¹

¹Kobe University Graduate School of Medicine, Department of Radiology, Kobe, Japan,

²Toshiba Medical Systems Corporation, Otawara, Japan

Purpose: To evaluate the effect of a new denoising technique, called adaptive iterative dose reduction (AIDR), for quantitative evaluation of pulmonary emphysema on low-dose CT as compared with evaluation on standard-dose CT.

Material/Methods: Standard-dose (150 mAs) and low-dose (25 mAs) thin-section CT images of 26 patients (20 men, 6 women; age, 57-84 years; smoking history, 0-180 pack-years), which had been acquired with a 16-detector-row CT scanner, were analyzed. Low-dose CT images were reconstructed without and with AIDR. As quantitative indices of emphysema, we calculated emphysema index and numbers of four emphysema clusters (cluster 1, 2-8mm³; cluster 2, 8-65mm³; cluster 3, 65-120mm³; cluster 4, < 120mm³) on low-dose CT without AIDR (LDCTm), low-dose CT with AIDR (LDCTp), and standard-dose CT (SDCT). To evaluate the effect of AIDR, we compared Bland-Altman 95% limits of agreement (LOA) between SDCT and LDCTm as well as SDCT and LDCTp.

Results: The LOA of emphysema index was: -0.084 to 0.055 between SDCT and LDCTm; -0.046 to 0.076 between SDCT and LDCTp. Effectiveness of AIDR was not apparent in emphysema index. On the other hand, the LOA of emphysema clusters were improved by AIDR, especially in small clusters. The LOA of clusters 1-4 were: -36200 to 5340, -8970 to 1750, -281 to 87.2 and -204 to 110 between SDCT and LDCTm; -7240 to 4220, -1790 to 1470, -127 to 98.0 and -146 to 117 between SDCT and LDCTp.

Conclusion: The new denoising technique can be useful for quantitative evaluation of emphysema on low-dose CT.

P63

Smoking-related interstitial lung diseases: Spectrum of HRCT features

Antunes V.B.^{1,2}, Meirelles G.S.P.¹, Szarf G.^{1,2}, Figueiredo C.M.¹, Maciel R.P.¹, Macedo-Neto A.C.¹

¹Fleury Medicina e Saude, São Paulo, Brazil, ²Universidade Federal de São Paulo - UNIFESP/EPM, São Paulo, Brazil

Purpose/aim: The purpose of this exhibit is to describe the spectrum of radiologic features of smoking-related interstitial lung diseases (ILD) with emphasis on high-resolution computed tomography (HRCT) findings.

Material/methods: Review of HRCT findings of the following diseases with sample cases:

- respiratory bronchiolitis and respiratory bronchiolitis-interstitial lung disease (RB-ILD)
- desquamative interstitial pneumonia (DIP)
- pulmonary Langerhans cell histiocytosis (PLCH)
- usual interstitial pneumonia / idiopathic pulmonary fibrosis (IPF).

Results: Cigarette smoking has been recognized as an important risk factor for the

development of several ILDs, including respiratory bronchiolitis, desquamative interstitial pneumonia, pulmonary Langerhans cell histiocytosis, and idiopathic pulmonary fibrosis. The main HRCT features of RB-ILD are poorly defined centrilobular nodules. Patients with DIP typically present diffuse ground-glass opacities and mild reticular pattern on HRCT. The coexistence of upper lung nodules and cysts in a smoker allows confident diagnosis of PLCH. The combination of lower lung fibrosis and upper lung emphysema is frequently observed in smokers, and it has been shown that cigarette smoking is associated with a higher risk for IPF. Although some HRCT findings are suggestive of a specific diagnosis, the clinical and radiological features can overlap, and mixed patterns of disease frequently coexist in the same patient.

Conclusion: To understand and recognize the HRCT features of smoking-related ILD is crucial for the diagnosis, classification and prognosis of these patients. However, in some cases an integrated clinical, radiological, and pathological approach is necessary for accurate diagnosis.

P64

Oxygen enhanced magnetic resonance relaxometry in COPD & asthma patients - preliminary results

Triphan S.¹, Wolf U.², Anjorin A.³, Ley S.³, Breuer F.¹, Jakob P.^{1,4}

¹Research Centre Magnetic Resonance Bavaria e.V., Würzburg, Germany, ²Universität Mainz, Mainz, Germany, ³Universitätsklinikum Heidelberg, Heidelberg, Germany, ⁴University of Würzburg, Experimental Physics 5, Würzburg, Germany

Purpose: Due to the paramagnetic nature of Oxygen (O₂), the amount of dissolved O₂ effects the T₁ relaxation time of pulmonary blood. Thus, in healthy subjects T₁ in lung tissue is reduced by up to 10% when switching the breathing gas from room air (RA, 21% O₂) to 100% O₂. Since the decrease of T₁ is proportional to the fraction of oxygen in the breathing gas the oxygen uptake in the lung can be monitored.

Material/Methods: So far 14 patients (9 COPD, 5 Asthma) and 9 healthy volunteers were examined. MR data were acquired on a 1.5T Avanto System (SIEMENS) using an Inversion Recovery Snapshot FLASH sequence allowing for pixelwise quantification of T₁ in one slice within a 6s breathhold. T₁ maps were acquired in 9-10 coronal slices at RA and 100% O₂.

Results: The mean T₁ at RA and 100% O₂ were determined in the whole lung for each subject. On average T₁ dropped from 1122±131 (RA) to 1072±127 (100% O₂) (4.5% Reduction) for COPD patients and from 1171±94 (RA) to 1102±88 (100% O₂) (5.9% Reduction) for Asthma patients. T₁ in healthy subjects was found to be 1200±47 (RA) and 1104±44 (O₂) (8.4% Reduction), in good agreement with previously reported results.

Conclusion: In this study, both the average T₁ at RA and the T₁ reduction due to breathing pure O₂ were significantly lower in COPD patients compared to Asthma patients and healthy volunteers. To gain statistical confidence, in the future more patients will be included in this study.



P65

Various imaging features of thoracic sarcoidosis on chest CT and PET/CT

Rho J.Y.¹, Yoo S.M.¹

¹CHA Bundang Medical Center, CHA University, Radiology, Sungnam-si, Korea, Republic of

Purpose: We described the various imaging features of thoracic sarcoidosis on chest CT and PET/CT, identifying those findings that may help to reach an initial or differential diagnosis.

Materials and methods: We retrospectively reviewed 10 patients (4 men, 6 women; age ranges of 28~66 years) with pathologically proven thoracic sarcoidosis from November 2007 to September 2010 on chest CT scan. A total of 2 PET/CT scan examinations were performed in 10 patients with CT scan. **Results:** On chest CT scan, eight patients had symmetric bilateral hilar and mediastinal lymphadenopathy (LAP) with pulmonary parenchymal abnormality. In four patients of the eight patients, typical pulmonary infiltrates (perilymphatic distributed micronodules/interstitial thickening) were present. In one patient, coalescent nodules (patchy airspace consolidation) and typical pulmonary infiltrates were present. In two patients, variable sized multiple well-defined nodules were present. In one patient, irregular solitary nodule and pleural effusion were present. One patient had symmetric bilateral hilar and mediastinal LAP without pulmonary parenchymal abnormality. One patient had typical pulmonary infiltrates without LAP. In two patients of nine patients with LAP, abdominal LAP was present. In two patients with PET/CT scan, strong FDG uptakes in LAP and irregular solitary nodule with LAP were seen.

Conclusion: In most cases with thoracic sarcoidosis, the characteristic feature was symmetric bilateral hilar and mediastinal LAP, with or without concomitant pulmonary parenchymal abnormality. However, the imaging findings of pulmonary parenchymal abnormality were nonspecific or atypical in some cases. It is important to consider various radiological findings associated sarcoidosis for correct diagnosis.

P66

TGF-beta-Inhibition in radiation-induced pulmonary fibrosis

Flechsig P.¹, Lahn M.², Dadrich M.¹, Peschke P.³, Bock M.³, Wirkner U.³, Abdollahi A.³, Kauczor H.-U.¹, Huber P.³

¹University Hospital Heidelberg, Diagnostic Radiology, Heidelberg, Germany,

²Lilly and Company, Frankfurt, Germany, ³DKFZ, Heidelberg, Germany

Materials and methods: The thoraces of C57BL/6 mice were irradiated with 20 Gy single dose, and a small molecule receptor tyrosine kinase inhibitor (RTKI) for TGF-beta-receptors 1, 2 was administered for a period of 20 days starting either before or after irradiation. The progression of pulmonary fibrosis in mice was monitored by volume-computed tomography, MRI and histological examination for up to 6 months.

TGF-beta-signaling alteration was analyzed by IHC.

Results: The histological examination showed, that the inhibition of TGF-beta signaling significantly reduced the induction of pulmonary fibrosis after 20 Gy thoracic radiation mice. There was no statistically significant difference, whether administration of the compound started before or after irradiation. Accordingly, MRI and volume-CT qualitatively showed a strong decrease of radiation-induced lung fibrosis development, while the CT additionally showed a quantitative reduction of lung density in drug treated mice vs. irradiation only.

Conclusions: Our findings underline the pivotal role of TGF-beta in the pathogenesis of radiation-induced pulmonary fibrosis. Moreover the data suggest, that the inhibition of TGF-beta signaling using small molecule RTKI can clinically be used to attenuate radiation-induced lung fibrosis. The study may point the way to a potential new treatment option of radiotherapy-related forms of lung fibrosis or fibrosis in other organs.

P67

Asbestosis: Radiologic and CT findings

Kim J.S.¹

¹Dongguk University Ilsan Hospital, Radiology, Goyang-si, Korea, Republic of

Purpose: The purpose of this exhibition is to show the imaging findings and the differential diagnosis of asbestosis.

Materials & methods: We reviewed the radiographic and CT findings, and the differential diagnosis of asbestosis in people who were exposed to asbestos.

Results: The main radiographic finding of asbestosis is bilateral small irregular opacities in the lower lung zones. CT findings are subpleural dotlike opacities, subpleural curvilinear opacities, intralobular interstitial and interlobular septal thickening, parenchymal bands, honeycombing and ground-glass opacity in conjunction with traction bronchiectasis.

Conclusion: Asbestos-related pulmonary and pleural disease is one of the important occupational lung diseases. Asbestos has been used widely since the 1970s in Korea and the prevalence of asbestos-related pulmonary and pleural complications has been increasing steadily. Recognition of the imaging features of asbestos-related diseases is important. Interstitial lung diseases, especially IPF (idiopathic pulmonary fibrosis) is well known and imaging features of IPF are similar to those of asbestosis, therefore better recognition of the imaging features of asbestosis is necessary for diagnosis.

P68

The importance of a standardized delicate CT follow-up protocol for long-term survival of lung transplant recipients. Twenty five cases review. Single centre experience.

Kudrnova S.¹, Kováts Z.², Müller V.², Balázs G.³

¹Semmelweis University Heart Centre, Diagnostic and Interventional Radiology, Budapest,



Hungary, ²Semmelweis University Pulmonology Clinic, Budapest, Hungary, ³Semmelweis University Heart Centre, Diagnostic Radiology, Budapest, Hungary

Purpose: Lung transplantation constitutes an ultimate treatment strategy in end-stage lung disease. Despite increasing number and improving survival-time of lung transplant recipients thanks to surgical innovations and revised recommendations for candidates' selection, long-term results are still unsatisfactory compared to other solid organ transplantations. Infections and chronic allograft dysfunction (BOS) represent the main culprits. Early detection and prompt treatment of both early and late post-operative complications are crucial for long-term survival. Since the early clinical and radiological manifestations are often very subtle, non-specific, even confusing, while lung transplant recipients are usually immune-suppressed, young and dyspneic, fast, sensitive, specific but non-invasive, multi-repeatable and organ-sparing are essential. Through our dedicated CT-protocol experience we would like to contribute to improved cost-benefit-risk balanced vital comprehensive follow-up care.

Materials/Methods: We have been following-up 15 lung recipients since June 2009. 37 dedicated examinations (1-6-12 months post-LTX routine, acute, treatment control) were performed. Our protocol: native (interstitial changes), pulmonary CTA (small circuit optimized arterial 1.5ml/kg 370mg I/ml i.v. CE), thin (1mm) slice spiral CT chest scan in inspiration, then low dose expiration scan (air-trapping). Especially patency of anastomoses, vascular, airway and parenchymal pulmonary structures, lymph nodes were evaluated, inflammatory changes investigated.

Results: Among significant pathology pulmonary artery and bronchus stenosis, bullous-cystous changes, bronchiectasis, mosaic perfusion, aspergillus infection confirming multifocal nodules and ground-glass opacities, air-trapping and atelectasis were identified enabling prompt appropriate therapy.

Conclusion: Through enabling prompt precise diagnosis as well as treatment adequacy control our delicate CT-protocol repeatedly significantly contributed to complex follow-up crucial for lung transplants' survival.

P69

Cystic lung disease: Differential diagnosis

Bento da Silva T.K.¹, Lorenzoni C.A.², Zanardo A.P.³, Bello R.M.¹

¹Mãe de Deus Hospital, Thoracic Radiology, Porto Alegre, Brazil, ²PUCRS, Porto Alegre, Brazil, ³Moinhos de Vento Hospital, Porto Alegre, Brazil

Purpose: The pulmonary cysts are part of the radiographic appearance of certain diseases. Cyst, by definition, is a well-defined rounded lesion, often with thin walls (< 2mm). It generally contains air, but can also be filled with inflammatory/infection exudate. This entity should be differentiated from other air space lesions, such as emphysematous bullae, excavated nodules and pneumatoceles.

Material and methods: We describe the main radiological findings, clinical and

pathological correlation of diseases that may develop lung cysts. To exemplify these diseases, we used imaging of patients of our hospital, with emphasis on computed tomography (CT) scan technique with high resolution.

Results: Cystic lung diseases share the presence of subpleural or intraparenchymatous radiolucent images, and may be focal or diffuse. The CT is more sensitive than plain radiograph, contributing significantly to the investigation of pulmonary cysts. These findings may be typical of a disease or be a rare form of presentation. The following conditions were analyzed: interstitial lymphocytic pneumonia, desquamative interstitial pneumonia, hypersensitivity pneumonitis, metastasis, pneumocystosis, amyloidosis, histiocytosis X and lymphangioleiomyomatosis.

Conclusion: Knowing the main pathologies that may manifest as pulmonary cysts is essential for the proper formulation of differential diagnoses and, consequently, to improve clinical research.

P70

CT operability evaluation of chronic thromboembolic pulmonary hypertension

Willeminck M.J.¹, van Es H.W.¹, Koobs L.¹, Morshuis W.J.², Snijder R.J.³, van Heesewijk J.P.M.¹

¹St. Antonius Hospital, Radiology, Nieuwegein, Netherlands, ²St. Antonius Hospital, Cardio-Thoracic Surgery, Nieuwegein, Netherlands, ³St. Antonius Hospital, Pulmonary Disease, Nieuwegein, Netherlands

Objective: The educational objectives of this article are to provide an overview of the CT findings in chronic thromboembolic pulmonary hypertension (CTEPH) and to improve the evaluation of operability.

Diagnostic CT Features: CT features of CTEPH can be classified in vascular signs and parenchymal signs. Vascular signs include direct signs of chronic pulmonary thromboembolism (complete obstruction and partial filling defects), signs due to pulmonary hypertension (central pulmonary dilatation, right ventricular enlargement and flattening and bulging of the ventricular septum to the left side) and signs due to collateral systemic supply (enlarged bronchial and nonbronchial systemic arteries). Parenchymal signs include mosaic lung perfusion pattern and pulmonary infarction.

Evaluation of Operability: CTEPH is surgically curable by pulmonary endarterectomy (PEA), in which the complete intima of the pulmonary artery including all obstructions is removed as completely as possible. The most important determinants of operability are the location and extent of the proximal thromboembolic obstruction. Distally localized thrombi are not accessible for PEA, only thrombi localized in the main, lobar or proximal segmental arteries are operable. Furthermore CT has a role in determining the status of the pulmonary parenchyma in patients with coexisting obstructive or restrictive lung disease, because severe underlying lung disease is a contraindication to PEA.

Conclusion: In this article we reviewed the key imaging findings on CT in patients with CTEPH. After completing, the reader should have an improved ability to



recognize these CT imaging findings and to make a decision whether the patient is operable or inoperable.

P71

Thoracic thin-section CT manifestations of myeloperoxidase-antineutrophil cytoplasmic antibody-related disease

Honda K.¹, Okada F.¹, Ando Y.², Ono A.¹, Nakayama T.¹, Kiyosue H.¹, Matsumoto S.¹, Mori H.¹, Vasculitis

¹Oita University, Oita, Japan, ²Nishibeppu National Hospital, Beppu, Japan

Purpose: No previous studies have described the CT findings in patients with elevated serum myeloperoxidase-antineutrophil cytoplasmic antibody (MPO-ANCA) who do not fulfill the criteria for microscopic polyangiitis (MPA), Churg-Strauss syndrome (CSS), and crescentic glomerulonephritis (CrGN). Therefore, the present study was undertaken to evaluate the CT findings in patients with elevated serum MPO-ANCA who do not fulfill the criteria (unclassified patients) in comparison with patients who do fulfill the criteria (classified patients).

Materials and methods: We retrospectively assessed thin-section CT images in 87 patients with elevated serum MPO-ANCA who underwent CT scans between January 2005 and March 2010. Our study population comprised 45 classified patients (21 men, 24 women; age range 25-89 years; mean age 68 years) with MPA (n=26), CSS (n=7), and CrGN (n=12) and 42 unclassified patients (14 men, 28 women; age range 17-98 years; mean age 67 years).

Results: Among the 45 classified patients, ground-glass opacity was observed most frequently, followed by traction bronchiectasis, honeycombing, and interlobular septal thickening. Among the 42 unclassified patients, the most common CT finding was ground-glass attenuation, followed by honeycombing, traction bronchiectasis, and interlobular septal thickening. Honeycombing was significantly more frequently observed in the unclassified patients than in the classified patients ($P < 0.05$). Bronchial wall thickening and pleural effusion were significantly more frequently observed in the classified patients than in the unclassified patients ($P < 0.05$ for each).

Conclusions: There were differences in the frequencies of honeycombing, bronchial wall thickening, and pleural effusion between the classified and unclassified patients.

P72

Visualization of dilated bronchial arteries using contrast-enhanced magnetic resonance angiography in cystic fibrosis patients - correlation to parenchymal lung changes

Optazaite D.-E.¹, Eichinger M.¹, Kopp-Schneider A.², Niemann A.³, Mall M.⁴, Kauczor H.-U.⁵, Puderbach M.⁶

¹German Cancer Research Center, Division of Radiology, Heidelberg, Germany, ²German

Cancer Research Center, Division of Biostatistics, Heidelberg, Germany, ³Heidelberg University Hospital, Department of Pediatrics, Heidelberg, Germany, ⁴University of Heidelberg, Department of Pediatrics, Heidelberg, Germany, ⁵University of Heidelberg, Department of Diagnostic and Interventional Radiology, Heidelberg, Germany, ⁶Thoraxklinik, University of Heidelberg, Department of Diagnostic and Interventional Radiology, Heidelberg, Germany

Introduction: The dilatation of bronchial arteries (BA) is a frequent cause of massive haemoptysis in patients with advanced cystic fibrosis (CF) and is associated with high morbidity and mortality. Therefore, visualisation of dilated BA is of great clinical significance for evaluation of CF-disease severity and planning of interventions. The aim of this study was to establish a magnetic resonance angiography (MRA) based method for assessment of BA in CF-patients and to correlate the number and degree of dilated BA with the severity of parenchymal lung changes.

Methods: 40 CF-patients with stable CF lung disease were examined by morphological (HASTE, VIBE) and functional (contrast enhanced MR-perfusion) MRI. Lung changes were assessed evaluating the bronchiectasis/wall thickening, mucus plugging, abscesses/sacculations, consolidations, pleural findings and perfusion defects. BA were visualized by contrast enhanced three-dimensional fast-low-angle shot pulse sequence and assessed by semi-quantitative score.

Results: Dilated BA were visible in patients with moderate and advanced lung parenchymal changes. In contrast, no bronchial arteries were detectable in patients with no or minor lung parenchymal changes. The degree and number of dilated BA correlated significantly with the severity of parenchymal lung changes ($r=0.602$; $p < 0.001$).

Conclusion: In the present work we established a new MRA-based method for visualization of bronchial arteries. Our data suggest that MRA based assessment of BA is of value for evaluation of CF-disease severity and provides important anatomical information for possible interventions. Therefore, we propose that BA MRA should be performed in advanced CF lung disease.

P73

Effectiveness of a radiologic warning system when a thoracic neoplasm is suspected

Tilve Gómez A.¹, Leiro Fernández V.², Botana Rial M.², Gil Gallego J.C.¹, Pallarés Sanmartín A.³, Rodríguez Paz C.¹, García-Tejedor J.L.¹, Fernández Villar A.²

¹Complejo Hospitalario Universitario de Vigo, Radiology, Vigo, Spain, ²Complejo Hospitalario Universitario de Vigo, Respiratory Medicine, Vigo, Spain, ³Complejo Hospitalario de Pontevedra, Respiratory Medicine, Vigo, Spain

Introduction: Two years ago we created a warning system from radiology department to respiratory medicine department when a lung cancer is suspected.

Materials and methods: Prospective study (december 2008-november 2010).



We included patients with radiological studies that were reported as suspected thoracic cancer. The method of notice from radiologists to chest physicians was the corporate email. Chest physicians contacted with the doctor who requested the chest radiography and he sent the patient to the respiratory medicine department.

Results: We included 118 patients, 82 (69.5%) males, median age 65 (interquartile range: IQR 54-76) years old. 84 (71.2%) patients were studied at our hospital. Most studies came from primary health (73.7%).

The most frequent radiological finding were: lung mass (42.4%), lung nodule (24.6%), pleural effusion (5.9%) and atelectasis (7.6%). 6.8% of the patients had several lesions. The median of days we needed to find the doctor was 1 (IQR 1-2) and to get a diagnosis 13 days (IQR 8-28).

81 patients ended the study, 49 (41.5%) patients had a diagnosis of malignancy (40 lung cancers, 5 metastasis, 3 mediastinal mass and one mesothelioma). Most were stage IV (11.9%) and IIIB (7.6%).

Bronchoscopy was the most frequent diagnosis method (26.3%), others were thoracic surgery (7.6%), transthoracic puncture (7.6%) and pleural biopsy (2.5%).

If only chest physicians were involved in the diagnosis the median days to get it was 10 (IQR 7-19).

Conclusions: A warning system from radiology department get a quick diagnosis in most patients with a suspected lung cancer.

P74

Poster withdrawn

P75

Combined Pulmonary Fibrosis and Emphysema: Clinical, pathological and radiological aspects

Winklehner A.¹, Fretz G.², Vogt P.³, Russi E.², Frauenfelder T.¹

¹University Hospital of Zurich, Institute of Diagnostic Radiology, Zurich, Switzerland,

²University Hospital of Zurich, Division of Pulmonary Medicine, Zurich, Switzerland,

³University Hospital of Zurich, Department of Clinical Pathology, Zurich, Switzerland

Purpose: The purpose of this poster presentation is the description of Combined Pulmonary Fibrosis and Emphysema (CPFE), in terms of clinical, pathological and radiological aspects, with emphasis on high-resolution CT (HRCT) imaging features.

Materials and methods: We analyse the main clinical, pathological and imaging findings of CPFE, with sample cases. Imaging aspects of CPFE on HRCT are reviewed and illustrated.

Results: The following findings are described and illustrated: 1) Subnormal spirometry and strongly impaired gas exchange, 2) high prevalence of pulmonary hypertension, 3) centrilobular and/or paraseptal emphysema with upper zone predominance, 4) fibrotic

changes of the lower lobes with associated honeycombing, reticular intralobular opacities and traction bronchiectasis.

Conclusion: The major teaching points of this poster presentation are: 1) CPFE is an underestimated rare entity, 2) familiarity with clinical and imaging aspects may help to accurately diagnose this syndrome.

P76

Poster withdrawn

P77

Effect of pulmonary fibrosis on pulmonary artery size in predicting pulmonary hypertension

Rajaram S.¹, Swift A.J.^{1,2}, Capener D.¹, Davies C.³, Hill C.³, Condliffe R.⁴, Hurdman J.^{2,4}, Elliot C.^{2,4}, Wild J.M.^{1,2}, Kiely D.G.^{2,4}

¹University of Sheffield, Academic Unit of Radiology, Sheffield, United Kingdom, ²Sheffield Cardiovascular Biomedical Research Unit, Sheffield, United Kingdom, ³Department of Radiology, Sheffield Teaching Hospitals Trust, Sheffield, United Kingdom, ⁴Royal Hallamshire Hospital, Sheffield Pulmonary Vascular Disease Unit, Sheffield, United Kingdom

Purpose: To determine the effect of pulmonary fibrosis on pulmonary artery size in predicting pulmonary hypertension (PH) .

Materials and methods: The transverse diameter of main pulmonary trunk (PA), right and left main pulmonary arteries (PA branch vessel) and aorto-pulmonary ratio (PA/Ao) were measured in 95 patients who underwent CT and right heart catheterization (RHC) for suspected PH. The mean age of the patients was 61 years with male to female ratio of 0.9. Based on degree of pulmonary fibrosis the patients were divided into group A (absent fibrosis or < 20% fibrosis) and group B (≥ 20% fibrosis). Mean pulmonary artery pressure (mPAP) and pulmonary vascular resistance (PVR) were obtained from RHC.

Results: Patients in group A (n=59) showed good correlations between PA size and PA/Ao ratio with mPAP (PA size: $r = 0.58$ $p < 0.0001$, PA/Ao ratio: $r=0.51$ $p=0.0002$) and PVR (PA size: $r = 0.52$ $p < 0.0001$ and PA/Ao ratio: $r=0.49$ $p < 0.003$). In contrast, for patients in group B (n=35), there was no significant correlation between PA size with mPAP ($r = 0.36$ $P < 0.017$) and PVR ($r = 0.27$, $P = 0.12$) and PA/Ao ratio showed only a weak correlation with mPAP ($r=0.44$ $p < 0.05$) and PVR ($r=0.32$ $p=0.05$). The PA branch vessel was not significant in either group.

Conclusion: In the absence of significant fibrosis, PA size is a better indicator of PH than PA/Ao ratio or PA branch vessel. However, in patients with fibrosis, PA size does not predict the presence of PH.



P78

Air trapping is a major determinant of treatment refractory - persistent airway obstruction in asthmatics; Follow-up study using High -Resolution CT

Park J.S.¹, Paik S.H.¹, Jeong S.H.¹, Park S.W.², Park C.S.²

¹Soonchuhyang University Bucheon Hospital, Radiology, Bucheon, Korea, Republic of,

²Soonchuhyang University Bucheon Hospital, Division of Allergy and respiratory Medicine, Department of Internal Medicine, Bucheon, Korea, Republic of

Purpose: Chronic persistent airway obstruction has been frequently observed in moderate to severe asthmatics despite prolonged treatment with higher dosages of inhaled corticosteroids. We investigated which airway changes were associated with this obstruction.

Materials/Methods: HRCT was performed at study entry and reexamined at the time of follow-up when the FEV1 reached a maximally constant level after treatment for 1 year or more with inhaled corticosteroids. FEV1 was measured regularly over 12 months. Bronchial wall area (WA) and air trapping (AT) extent were compared in the recovered group (RG) (n = 18) and the persistent-airway-obstruction group (PAOG) (n = 14).

Results: WA and AT of the initial HRCT were similar between the two groups. On follow-up HRCT, AT was markedly decreased in the RG compared with that on initial HRCT ($P = 0.017$), whereas BWA did not change ($P = 0.34$). In the PAOG, these two parameters did not change during follow-up. When follow-up HRCT was compared, AT was significantly greater in the PAOG than in the RG ($P = 0.003$). dpost-BD FEV1 was correlated with dAT(%) on the follow-up HRCT ($P = 0.017$). The presence of persistent airflow obstruction were significantly associated with the AT% difference between initial and 2nd time (RR=1.70, $P=0.018$).

Conclusions: Persistence of AT could be a main contributing factor to chronic persistent airflow obstruction in MSBA.

P79

Maximum standardized uptake value of the primary tumor, T1a, T1b, T2a and T2b of non small cell lung cancer, according to 7th IASLC staging

Yi J.G.¹, Park S.H.¹, Park J.H.¹

¹Konkuk, Radiology, Seoul, Korea, Republic of

Purpose: We want to know whether the maximum standardized uptake value (mSUV) of non small cell lung cancer is significantly different between T staging of 7th IASLC.

Materials and methods: This is a retrospective review of CT and surgical data of T descriptor from classic TNM system (T1, T2) to new staging (T1a, T1b, T2a, T2b). 39 patients (M:F = 28:11, mean age, 58) were grouped as T1a, T1b, T2a, and T2b (Number of patients = 15, 13, 9, 2), irrespective of N staging, according to axial CT measurement (mean tumor size on CT scans were 1.5, 2.4, 3.8, 6.3 cm) and all were histologically

proved during the period of May 2005 to Dec. 2009. T2b cases were excluded due to small number.

Results: Mean values of mSUV are 4.0, 6.1, 9.1 and SD of 2.7, 3.7, 4.5 each from T1a, T1b, and T2a groups. Mean mSUV of these three groups are significantly not same by ANOVA (p value = 0.007). Multiple comparison results from Duncan's grouping shows, mean mSUV of T1a and T2a is significantly different, but, not significantly different between T1a and T1b, also between T1b and T2a. By the way, mean mSUV of T1(T1a + T1b, N=28) and T2(T2a + T2b, N=11) according to previous staging are 5.0, 9.6 with significant difference (T test, p value = 0.0009).

Conclusion: Mean values of mSUV between new T1a and T1b, T1b and T2a are not significantly different, but significantly different between T1a and T2a groups.

P80

Fat-containing lesions of the mediastinum: imaging features and differential diagnosis

Chagas - Neto F.A.¹, Santos M.K.¹, Hernandez M.A.¹, Barreto A.R.F.¹, Teixeira S.R.¹, Elias Jr J.¹, Muglia V.F.¹

¹School of Medicine of Ribeirao Preto - University of Sao Paulo, Radiology, Ribeirao Preto, Brazil

Purpose: Occasionally, mediastinal masses may have fat attenuation at computed tomography (CT) or characteristic signal intensity of fat at magnetic resonance imaging (MRI), which can abbreviate differential diagnosis. We aimed to discuss and illustrate CT and MRI features of fat-containing lesions in the mediastinum.

Materials and methods: We retrospectively reviewed CT and MRI exams of patients with fat-containing lesions in the mediastinum, obtained in our institution between 2005 and 2011. Most interesting cases were selected for discussion and presentation of the imaging characteristics and major differential diagnosis.

Results: Some fat-containing mediastinal lesions are described: thymolipoma, mediastinal lipomatosis, liposarcoma and chondrosarcoma, lipomatous hemangiopericytoma, lipomatous hypertrophy of the interatrial septum and Morgagni's diaphragmatic hernia. All cases have surgical or pathological confirmation. Most important imaging features in CT and MRI are discussed, like location, morphology, fat characterization and distribution, post contrast enhancement and others.

Conclusions: CT and MRI are exceedingly valuable in the evaluation of lesions of the mediastinum. When a fat-containing lesion is identified, description of its location and other imaging features significantly shortens the differential diagnosis, helping not only to distinguish between benign and malignant lesions, but sometimes also offering a radiologic definite diagnosis.



P81

MRI evaluation of chest tumors, including lungs and heart: case series and review

Santos M.K.¹, Schmidt A.², Trad H.S.¹, Muglia V.F.¹, Elias Jr J.¹

¹School of Medicine of Ribeirao Preto - University of Sao Paulo, Radiology, Ribeirao Preto, Brazil, ²School of Medicine of Ribeirao Preto - University of Sao Paulo, Cardiology, Ribeirao Preto, Brazil

Purpose: Provide an overview of the role of magnetic resonance imaging(MRI) in the evaluation of chest tumors, including cardiac and pulmonary lesions, reviewing a series of cases; and to discuss current techniques and diagnostic criteria to limit differential diagnosis.

Materials and methods: MRI exams of patients scanned in our institution, for thoracic mass lesions investigation, were retrospectively reviewed. Images were acquired in 1.5T systems, using body and torso coils and specific sequences, including T1 and T2 weighted images, with and without fat suppression, pre and post gadolinium. Cardiac lesions were studied with ECG-triggered dedicated protocols.

Results: 60 patients were reviewed, with: 27(45%) mediastinal masses, 13(21%) chest wall lesions, 13(21%) masses involving lungs or pleura and 7(11%) heart tumors. Most lesions were primary, except for 9(15%) metastatic ones. Most common lesions included tymphic hyperplasias and other benign lesions in mediastinum, lymphangiomas in chest wall, lung metastasis and primary carcinomas, and cardiac atrial mixoma.

More rare lesions were also described, as cardiac sarcoma, fibroma and rhabdomyoma, pleuropulmonary blastoma, ectopic parathyroid, breast sarcoma and thoracic hydatidosis.

Conclusions: MRI is traditionally demanded for the evaluation of chest wall and mediastinal masses, but recent advances in acquisition techniques have allowed to evaluate lesions in other locations, like in the heart and lungs, with good conspicuity. Such advances include use of parallel imaging, data partial acquisition, accurate synchronization mechanisms and new body fast imaging sequences. MRI can define tumor location and tissue characteristics, narrowing the differential diagnosis of chest masses, including cardiac and pulmonary ones.

P82

Neuroendocrine tumors of the lung: case series with histopathologic correlation and focus on CT findings

Barreto A.R.F.¹, Chagas - Neto F.A.¹, Muglia V.F.¹, Elias Jr J.¹, Santos M.K.¹

¹School of Medicine of Ribeirao Preto - University of Sao Paulo, Radiology, Ribeirao Preto, Brazil

Purpose: Neuroendocrine tumors of the lung(NTL) arise from the bronchial mucosa and

are currently classified in: typical carcinoid, atypical carcinoid, large cell neuroendocrine carcinoma (LCNC) and small cell lung cancer (SCLC). We aimed to describe and discuss imaging findings in a series of cases of NTL.

Materials and methods: We retrospectively reviewed imaging exams in patients with NTL diagnosed in our institution in the last few years, all cases with histopathologic confirmation, focusing on CT findings.

Results: Images of 19 patients were reviewed, comprising: 3 typical carcinoids, 2 atypical carcinoids, 3 LCNC and 11 SCLC. One typical carcinoid presented at CT as a central endobronchial nodule with distal atelectasis (classical description) and the other two were found as homogeneous pulmonary nodules; atypical carcinoids were described as well delimited peripheral masses, with heterogeneous enhancement, one containing calcifications; two LCNC lesions were found as masses similar to the atypical carcinoids and one as a central infiltrative lesion; and SCLC cases were described mostly as large infiltrative central masses, heterogeneous and ill defined, associated with thoracic lymphadenopathy and secondary lesions (most common presentation). One SCLS had a different aspect, presenting as a well-defined rounded paramediastinal mass, without lymphadenopathy. One typical carcinoid was also studied with magnetic resonance imaging.

Conclusions: Although there are some less specific and other overlapping imaging features between the NTL, integration of the clinical data and imaging findings, especially at CT, may be useful in differentiation of the different subtypes of pulmonary neuroendocrine tumors, helping to optimize treatment options.

P83

Pseudocavity on pulmonary infarction

Mazon M.¹, Domingo M.², Miralles S.², Leiva C.³, Flors L.³, Vilar J.²

¹H. U. Dr. Peset, Radiology, Valencia, Spain, ²H. U. Dr. Peset, Valencia, Spain, ³H. U. La Fe, Valencia, Spain

Purpose: To assess the frequency and specificity of pseudocavity in pulmonary infarction and compare them in other pathologies.

Materials and methods: We define pseudocavity as an oval or rounded areas of lucencies in mediastinal window, it represents spared parenchyma, with interlobular septal thickening and ground glass opacity in lung window .

Two thoracic radiologists retrospectively analyzed 150 CT images, 75 pulmonary infarctions and 75 other consolidations of other etiologies, selected by an independent radiologist. Pseudocavitation presence, subpleural location and morphology were analyzed. Frequency, sensitivity, specificity, and positive likelihood ratio were calculated.

Results: 150 CT images were analyzed in 100 patients (45 men 55 women, mean age of 62.2 years \pm 15.1 vs 66.9 \pm 18.4; $P=$.09).

Infarction had a higher frequency of triangular shape 40 vs 17.3 % (30/75 vs 13 of 75) $P=$.002, pseudocavitation 41.3 vs 21.3 % (31/75 vs 16/75) $P=$.008, and subpleural



location 86.7 vs 58.7% (65/75 vs 44/75) $P=$.001. Positive LR was 3.18 for triangular shape, 2.6 for pseudocavitation, and 4.58 for subpleural location, 1.3 for triangular shape. Presence of triangular shape had 98% specificity and 46% sensitivity for pulmonary infarction, pseudocavitation had 78% specificity and 41% sensitivity, and subpleural localitation had 41% specificity and 86% sensitivity. Pseudocavitation showed 93% specificity and 49% sensitivity, and when combined with triangular shape specificity increased to 96% specificity but sensitivity decreased to 25%

Conclusion: The presence of pseudocavitation and triangular shape suggests pulmonary infarction. A combination of these features increases the specificity but decreases the sensitivity.

P84

Effects of chronic obstructive pulmonary disease on thoracic vascular calcifications

Jobst B.J.¹, Owsijewitsch M.¹, Becker N.², Delorme S.³, Ley S.¹, Ley-Zaporozhan J.¹, Heussel C.P.⁴, Kopp-Schneider A.⁵, Puderbach M.^{3,4}, Kauczor H.-U.¹

¹University of Heidelberg, Department of Radiology, Heidelberg, Germany, ²DKFZ Heidelberg, Division of Cancer Epidemiology, Heidelberg, Germany, ³DKFZ Heidelberg, Department of Radiology, Heidelberg, Germany, ⁴Thoraxklinik Heidelberg, Department of Radiology, Heidelberg, Germany, ⁵DKFZ Heidelberg, Division of Biostatistics, Heidelberg, Germany

Purpose: Recent epidemiological evidence suggests that impaired lung function and emphysema in patients with COPD are risk factors for cardiovascular disease due to systemic inflammation. We tested the hypothesis that COPD is a risk factor for cardiovascular calcifications, independent of tobacco use.

Materials and methods: 200 patients with COPD at different GOLD-stages (at risk, GOLD I-IV) were included in the study (median age 60 years, 129 males, 71 females). The overall volume of thoracic vascular calcifications (thoracic aorta, coronary arteries, supraaortic branches, and aortic valve) was determined by applying a volume score on low dose ungated MDCT scans. Axial slices within a region from T1 through T12 were taken into account. Effects of smoking history, gender, age, BMI, GOLD-stage, and emphysema index on vascular calcifications were determined by stepwise multiple linear regression analysis.

Results: Median value of overall calcium was 988.5 mm³, of BMI 25.2, of smoking history 40.0 PY, and of emphysema index 0.196. The regression analysis revealed that age ($p < 0.001$), GOLD-stage ($p < 0.001$), and BMI ($p = 0.026$) were linked to the overall volume of calcifications. The increase in r^2 was 0.231 for age, 0.052 for the GOLD-stage and 0.018 for BMI. (Regression function: overall p -value < 0.001 ; $r^2 = 0.302$).

Conclusion: In our cohort, COPD-stage and BMI are significant predictors of thoracic vascular calcifications, while age seems to be best predictor. Among the tested COPD criteria, emphysema index, smoking history, and gender did not show statistical significance.

P85

Bronchopulmonary Dysplasia: Evaluation of abnormalities of lung structure using Hyperpolarized Helium-3 diffusion-weighted MRI

Flors L.¹, Mata J.¹, Froh D.K.², Paget-Brown A.², de Lange E.E.¹, Mugler III J.P.¹, Wang C.¹, Altes T.A.¹

¹University of Virginia Health System, Radiology, Charlottesville, United States,

²University of Virginia Health System, Pediatrics, Charlottesville, United States

Purpose: To determine the ability of Hyperpolarized (HP) ³He diffusion-weighted MRI in detecting abnormalities in lungs of children with BPD.

Materials/Methods: HP ³He diffusion-weighted MRI was performed in 19 subjects with history of preterm-birth and BPD (age range 5-14 years; mean 8.57 years) and 29 healthy term-birth subjects (4-14 years; 8.82 years). Coronal images were acquired with two b values, 0 and 1.6 s/cm², using a gradient-echo sequence with bipolar diffusion gradients. The mean ADC from the whole lung and the percent of the lung volume with ADC > 0.2 cm²/s were calculated. The mean ADC of all subjects was corrected for age using the linear regression coefficients of the mean ADC vs age curve from healthy subjects.

Results: The mean ADC was significantly greater for the BPD patients (0.185 cm²/s) than for the healthy subjects (0.152 cm²/s), $p = 0.001$. After correcting for age, the mean ADC remained elevated for BPD (0.203 cm²/s) relative to the healthy subjects (0.168 cm²/s), $p < 0.001$. The mean percent of the lung volume with an ADC > 0.2 cm²/s was 31% for BPD and 12% for healthy, $p < 0.001$. The ventilated lung volume from the MR images was similar for the subjects with BPD (1.9L) and the healthy subjects (2.1L), $p = 0.43$.

Conclusion: Children with BPD had elevated ADC values, suggestive of enlarged alveoli, and the same lung volumes as compared with age matched healthy control subjects. These findings are consistent with the limited histological data demonstrating that children with BPD have enlarged alveoli that are reduced in number.

P86

Reduction of radiation - induced pulmonary fibrosis in a murine model by combined PDGF and TGF - β RTKI

Dadrich M.^{1,2}, Peschke P.², Wirkner U.², Flechsig P.^{1,2}, Jenne J.², Abdollahi A.², Bock M.³, Kauczor H.-U.¹, Huber P.²

¹University Hospital Heidelberg, Department of Diagnostic and Interventional Radiology, Heidelberg, Germany, ²DKFZ, Radiation Oncology, Heidelberg, Germany, ³DKFZ, Division of Medical Physics in Radiology, Heidelberg, Germany

Purpose: Radiotherapy for lung cancer may induce severe pulmonary damage because radiation tolerance of lung tissue is limited. We investigated the effect of an antifibrotic therapy consisting of receptor tyrosine kinase inhibitors (RTKI) Imatinib and SU9518 (PDGFR - α and - β) alone and in combination with an RTKI for TGF - β receptor (TGF -



β RTKI) in a murine model.

Materials/Methods: Thoraces of C57BL/6 mice were irradiated with a single dose of 20 Gy using a high energy photon beam (6 MeV). Antifibrotic therapy using SU9518, Imatinib and TGF - β - RTKI monotherapies and combination schedules started two weeks after irradiation. Anti - PDGF treatments were given until the end of observation (24 weeks) and anti - TGF - β therapy was given for 4 weeks. Histological analysis and non - invasive radiological monitoring using MRI, Volume - CT, and high resolution CT were performed before irradiation and 2, 12, 16, 20 and 24 weeks after irradiation.

Results: Radiation induced severe pulmonary fibrosis in all untreated mice. The first marked signs of fibrosis could be observed 12 weeks after irradiation, constantly deteriorating up to the endpoint after 24 weeks. Monotherapy with either compound markedly attenuated fibrogenesis and increased mouse survival in accordance with improved clinical status, histological analysis and radiological data from MRI, VCT and HRCT. Combined anti - PDGF and TGF - β regimen further improved the beneficial antifibrotic effects along all measured criteria.

Conclusions: Our data suggest that RTKI for PDGF and TGF - β are promising antifibrotic treatment options for radiation - induced lung fibrosis. Furthermore, the combined inhibition of both pathways is tolerable and has stronger antifibrotic effects than each monotherapy.

P87

Assessment of Pulmonary Vein Stenosis as a potential complication after Pulmonary Vein Isolation using CT- and MR-Angiography

Dornia C.¹, von Bary C.², Weber S.², Poschenrieder F.¹, Eissner C.², Fellner C.¹, Fredersdorf-Hahn S.², Stadler S.², Stroszczyński C.¹, Hamer O.W.¹

¹University Medical Center Regensburg, Department of Radiology, Regensburg, Germany,

²University Medical Center Regensburg, Department of Internal Medicine II, Regensburg, Germany

Purpose: Pulmonary vein stenosis (PVST) is a well-known complication after pulmonary vein isolation (PVI). Specifically designed ablation catheters for antral PVI may minimize the incidence of PVST. We investigate the incidence, severity and characteristics of PVST following PVI using CT- and MR-Angiography.

Materials and methods: 100 patients (54 males) underwent PVI for paroxysmal atrial fibrillation using the recently developed pulmonary vein ablation catheter (PVAC). Multidetector computed tomography (CT) or contrast-enhanced MR-angiography (MR) was performed in all patients prior to and 93 ± 78 days after PVI. PVST was classified as follows: insignificant (< 25 %), mild (25-50%), moderate (50-75 %) and severe (>75%). A total of 410 PVs were analyzed. Quality of images was assessed subjectively applying a 4 point score (inappropriate, minor, good, excellent).

Results: Cardiac imaging demonstrated a narrowing of the PV diameter in 23 (23%)

patients and in 28 (7%) PVs. In detail, insignificant PVST was observed in 12 (2,9%), mild PVST in 15 (3,7%) and moderate PVST in one (0,2%) PV. No severe PVST was found. Image quality was excellent or good in 100% (75/75) of CT scans and 90% (112/125) of MR scans. There were no inappropriate, non-diagnostic images.

Conclusions: PVST is a possible but rare complication following phased-RF ablation using the PVAC. Both, CT- and MR-Angiography emerged as excellent diagnostic tools to define the PV anatomy before and estimate possible PVST after PVI with a high level of image quality during routine imaging.

P88

Ventilation-based segmentation of the lungs using hyperpolarized ³He MRI

Flors L.¹, Tustison N.J.¹, Avants B.B.², Leiva-Salinas C.¹, Altes T.A.¹, de Lange E.E.¹, Mugler III J.P.¹, Gee J.C.²

¹University of Virginia Health System, Radiology, Charlottesville, United States, ²Penn Image Computing and Science Laboratory, University of Pennsylvania, Philadelphia, United States

Purpose: To evaluate the performance of an automated segmentation method to quantify the ventilated and non-ventilated lung volume on hyperpolarized (HP) ³He MR images.

Materials/Methods: HP ³He ventilation MR images of 18 subjects (4 healthy volunteers and 14 patients with cystic fibrosis) were retrospectively evaluated. Using HP ³He and ¹H MR image data, a trained radiologist segmented the entire lungs on the HP ³He MR images. Four human readers manually segmented the ventilation defects within the masked lung regions for all 18 subjects. A computational processing (CP) algorithm was also used to segment the ventilation defects. The CP consisted of the following 3 essential steps: 1) inhomogeneity bias correction, 2) whole lung segmentation, and 3) subdivision of the lung segmentation into regions of similar ventilation. Simultaneous truth and performance level estimation (STAPLE) algorithm was used to produce a probabilistic estimate of the ground truth segmentation for each of the subjects. Using this ground truth estimate, we compared the segmentations produced by each human reader and the CP algorithm.

Results: The STAPLE results yielded the following sensitivity/specificity numbers: CP (0.898/0.905), reader #1 (0.743/0.897), reader #2 (0.501/0.985), reader #3 (0.898/0.848), and reader #4 (0.600/0.984). Whereas CP took < 10 minutes to segment all 18 cases, the times taken by the human readers were about 7-10 hours.

Conclusion: Our results strongly indicate that the proposed algorithmic processing may be a reliable, automatic method for quantitating ventilation defects.

Acknowledgments: Funding from Fundacion Caja Madrid, Spain.



P89

4-Dimensional assessment of larynx with 320-slice dynamic volume CT: Diagnostic criterion of vocal cord dysfunction

Lau K.K.¹, Bardin P.², Low K.², Crossett M.¹

¹Monash Medical Centre, Diagnostic Imaging, Melbourne, Australia, ²Monash Medical Centre, Respiratory and Sleep Medicine, Melbourne, Australia

Introduction: Vocal cord dysfunction (VCD) is often misdiagnosed as steroid-resistant asthma and can co-exist with asthma in >30% cases. VCD responds to speech therapy treatment. The gold standard of diagnosing VCD is by direct invasive laryngoscopy which may not be readily available and does not quantify VCD. Dynamic volume 320-slice CT permits real-time viewing of vocal cord movement and becomes a non-invasive tool for the prompt diagnosis of VCD. The aim of this study is to define a CT diagnostic criterion that quantifies VCD.

Method: Dynamic non-contrast laryngeal CT's of the entire breathing cycle of 29 healthy subjects were performed. An analysis algorithm based on the mean ratios of transverse laryngeal dimensions at vocal cord level to transverse dimensions at 1st tracheal ring level (RATIOS) at every 0.35 seconds of entire breathing cycle was established.

CT's were then conducted on 46 difficult-to-treat asthmatics. The RATIOS were plotted against the algorithm and compared.

Result: No RATIOS of all 29 normal subjects were below 1.5 standard deviations (1.5 SD) under the mean during the breathing cycle.

50% of the 46 asthmatic subjects had co-existent abnormal vocal cord movements. Their RATIOS were below 1.5 SD under the mean: 12% on inspiration, 8% on expiration and 30% on both inspiration and expiration.

Conclusion: 50% of our asthmatic patients studied had co-existent VCD. Dynamic volume CT permits 4D non-invasive morphological assessment of vocal cords. This CT diagnostic criterion (1.5SD below the mean of RATIOS) would facilitate the detection of unsuspected or co-existing VCD.

P90

Bronchioloalveolar carcinoma: solitary pulmonary nodule presentation at CT.

Casula E.¹, Domingo Montañana M.L.¹, Vila Miralles R.¹, Cerverón Izquierdo M.J.¹, Miralles Soria S.¹, Pellicer de Gracia B.¹, Cabrera Orozco G.¹, Mazón Momparler M.¹, Vilar Samper J.¹

¹University Hospital Dr Peset, Radiology, Valencia, Spain

Purpose: To describe CT findings of bronchioloalveolar carcinoma when presenting as a solitary pulmonary nodule, including those radiological signs most specific for this entity.

Material/Methods: We reviewed the CT studies of 33 patients with a histologically confirmed diagnosis of bronchioloalveolar carcinoma in our center in a 3-year period.

The different forms of presentation were described. Special emphasis was made on the nodular presentation of BAC.

To quantitatively assess the relative lower density of bronchioloalveolar carcinoma, densities were compared between the consolidative form of bronchioloalveolar carcinoma and the non-tumoral consolidations in patients in our control group.

Results: A solitary pulmonary nodule, spiculated, with pleural tag and air bronchogram, with poorly defined contours and solid density has proved to be the most frequent form of presentation of bronchioloalveolar carcinoma. The CT-angiogram sign, which has been described in literature as specific for bronchioloalveolar carcinoma was present in only two of our patients.

No statistically significant differences were observed, obtaining a mean density of 25,5 between the consolidative form of bronchioloalveolar carcinoma and the non-tumoral consolidations .

Conclusion: Solitary pulmonary nodule is a frequent form of presentation of bronchioloalveolar carcinoma. As opposed to what has been previously described in literature, CT angiogram sign and low density were not proved to be specific for bronchioloalveolar carcinoma in our study.

A spiculated nodule with pleural tag and air bronchogram should raise the suspicion of bronchioloalveolar carcinoma, among other entities in the differential.

P91

MDCT of transvenous extension of pulmonary neoplasms to the left atrium

Loutfi S.¹, Khankan A.¹, Mohammed M.F.¹, Al Bassam W.¹, Al Ghanim S.¹, Al Moaiqel M.¹

¹King Abdulaziz Medical City, Medical Imaging, Riyadh, Saudi Arabia

Purpose: To demonstrate the imaging capabilities of Multidetector Computed Tomography (MDCT) in the diagnosis and characterization of primary and secondary pulmonary neoplasms extending to the left atrium via the pulmonary veins route.

Background: Cardiac metastases are far more common than primary neoplasms and can involve the heart through four pathways: Direct invasion, hematogenous spread, lymphatic dissemination and by transvenous propagation.

Transvenous extension to the left atrium through the pulmonary veins is rare and was reported in both primary bronchogenic carcinoma and pulmonary metastases.

Clinically, intracavitary metastases may present with shortness of breath, chest pain and arrhythmias.

Echocardiography displays left atrial mass that simulates intracardiac thrombus and atrial myxoma.

MDCT clearly depicts the intracardiac extension with high accuracy in addition to its multiplanar capabilities in the assessment and staging of the pulmonary origin of the cardiac mass.

Results: We present cases of both primary and secondary lung neoplasms propagating to the left atrium with emphasis on the role of MDCT in proper evaluation and assessment.



Conclusion: Intacavitary extension of pulmonary neoplasms to the left atrium is a rare phenomenon that may simulate primary cardiac neoplasms namely myxoma both clinically and echocardiographically.

MDCT is an important tool for the accurate detection of this extension which may have an important therapeutic implications and alters patient's management and outcome.

P92

Poster withdrawn

P93

Change of sizes of superior vena cava (SVC) at inspiration and expiration CT

Sakai F.¹, Takahashi M.¹, Nakajima R.¹, Tominaga J.¹, Kimura F.¹

¹Saitama International Medical Center, Saitama Medical University, Diagnostic Radiology, Hidaka, Japan

Purpose: On frontal X-ray, vascular pedicle width (VPW) is one of reliable indicators of circulatory blood volume. SVC size determines the width of VPW and VPW shows little change during respiratory cycle. Measurement of SVC dimension at CT may be useful to estimate circulatory blood volume; however what kind of factors may affect the dimension of SVC has not been fully investigated. Purpose of this study is to measure the change of SVC dimensions between at inspiration and expiration CT and to investigate reliability of measurement of SVC dimension at CT.

Subjects and methods: Our study group comprised 24 patients underwent CT at full inspiration and full expiration from two institutions. Dimension of SCV was measured in vertical and transverse diameters and surface of SVC above and below the insertion of azygos vein.

Results: Above the insertion of the azygos vein, ventrodorsal and transverse diameters, and surface area of SVC were 18.4mm, 12.0 mm, 181mm² at full inspiration, and 20.6mm, 16.1mm, 262 mm² at full expiration. At the level of the azygos vein insertion, ventrodorsal, transverse diameters and surface of SVC were 17.2mm, 14.0mm, 196mm² at full inspiration, 20.6mm, 16.1mm, 262 mm² at full expiration. At both levels, measurement of SVC dimensions at full expiration showed significantly larger than those at full inspiration ($p < 0.001$).

Conclusion: Size of SVC at CT are different during the degree of inspiration and we must be careful to rely on SVC dimension at CT when we estimate circulatory blood volume

P94

Swine-origin influenza A (H1N1) viral infection: thoracic findings on CT

Marchiori E.¹, Zanetti G.¹, D'Ippolito G.², Verrastro C.², Meirelles G.S.³, Capobianco J.⁴, Rodrigues R.⁵

¹UFRJ and UFF, Rio de Janeiro, Brazil, ²UNIFESP, Sao Paulo, Brazil, ³Fleury Medicina e Saude, Sao Paulo, Brazil, ⁴Hospital do Coracao, Sao Paulo, Brazil, ⁵D'OR Institute for Research and Education, Rio de Janeiro, Brazil

Purpose: The aim of this article was to illustrate various computed tomography (CT) manifestations in patients with swine-origin influenza A (H1N1) viral infection.

Material and methods: The authors review a large series of cases of H1N1 viral infection, with emphasis on the main parenchymal and extra-parenchymal findings of the disease on CT. The differential diagnosis with other diseases is also presented.

Results: The predominant CT findings of H1N1 infection are ground-glass opacities, areas of consolidation, or a mixed pattern of the two. The abnormalities are frequently bilateral, and may have a peripheral subpleural, peribronchovascular, lobular or a random distribution. Although none of these patterns is specific of the condition, the main patterns of disease that would be most suggestive of H1N1 are scattered lung consolidations and/or ground glass opacities in a peribronchovascular or subpleural distribution. Small pleural effusions, pulmonary emboli and cysts may also be seen.

Conclusion: The imaging findings of this infection include consolidations, ground-glass opacities, interlobular septal thickening, small nodules, and findings of small airway disease, among others. Definitive diagnosis is based on the correlation of CT findings with clinical symptoms and laboratory tests.

P95

Comparative study of clinical, pathological and HRCT findings of primary alveolar proteinosis and silicoproteinosis

Souza C.A.¹, Marchiori E.², Gonçalves L.P.³, Meirelles G.⁴, Zanetti G.³, Escuissato D.L.⁵, Capobianco J.⁶, Soares Souza Jr A.⁷

¹The Ottawa Hospital, Diagnostic Imaging, Ottawa, Canada, ²UFRJ and UFF, Rio de Janeiro, Brazil, ³UFRJ, Rio de Janeiro, Brazil, ⁴Fleury Medicina e Saude, Sao Paulo, Brazil, ⁵UFPR, Curitiba, Brazil, ⁶Hospital do Coracao, Sao Paulo, Brazil, ⁷FAMERP, Sao Jose do Rio Preto, Brazil

Purpose: To compare the clinical, HRCT and pathological findings of primary alveolar proteinosis (PAP) and silicoproteinosis.

Material and methods: The study included 15 patients with PAP and 3 with silicoproteinosis. PAP was diagnosed by lung biopsy in 13 and bronchoalveolar lavage in two patients and silicoproteinosis by bronchoalveolar lavage in 10 and autopsy in three cases. HRCT images were reviewed by two chest radiologists with consensus for the presence, extent and distribution of ground-glass opacities, septal thickening, consolidation and nodules. Radiological-pathological correlation was performed by one radiologist and one chest pathologist.

Results: Seven (46%) patients with PAP were asymptomatic; the remainder presented slowly progressive dyspnea and dry cough. All silicoproteinosis patients had dry



cough and rapidly progressive dyspnea. The most common HRCT finding on PAP was the crazy-paving pattern (93%). All cases had areas of geographic sparing in the affected lung. The most common finding in silicoproteinosis (92%) was dependent consolidation with calcification in 83%. Centrilobular nodules were common (85%). On pathology, both diseases demonstrated intra-alveolar accumulation of PAS material, thickening of interlobular septae and alveolar walls and no evidence of fibrosis. A few silica particles were seen in silicoproteinosis.

Conclusion: Despite the pathological similarities, PAP and silicoproteinosis have distinct clinical and imaging features and prognosis. Bilateral crazy-paving pattern with areas of geographic sparing is characteristic for PAP. Silicoproteinosis presents with bilateral dependent consolidation often with areas of calcification. The crazy-paving pattern is not seen in silicoproteinosis.

P96

Quantitative 3D-Micro-CT imaging of the human lung pathology

Kampschulte M.¹, Schneider C.R.¹, Litzlbauer H.D.¹, Schneider C.¹, Zeiner C.², Tscholl D.³, Krombach G.A.¹, Ritman E.L.⁴, Bohle R.M.², Langheinrich A.C.¹

¹University Hospital Giessen, Radiology, Giessen, Germany, ²University Hospital Homburg/Saar, Pathology, Homburg/Saar, Germany, ³University Hospital Homburg/Saar, Thoracic and Cardiovascular Surgery, Homburg/Saar, Germany, ⁴Mayo Clinic College of Medicine, Physiology and Biomedical, Rochester, United States

Purpose: Imaging of tissue proliferation and changes in microvasculature caused by vascular remodeling in interstitial lung diseases is limited by current multidetector CT. We evaluated micro-CT imaging of the human lung fine structure to quantify morphologic differences of different tissue alterations and give an image-based estimation for the needed resolution for imaging of pulmonary microvasculature in lung fibrosis.

Materials and methods: Using micro-computed tomography (micro-CT) and synchrotron based micro-computed tomography (syn-MCT) human lung specimens (n = 54 specimens) with lung fibrosis and centrilobular emphysema were scanned and compared to controls. Fibrotic specimens were scanned native and contrast enhanced. Specimens with emphysema were volume-controlled fixed and contrast enhanced. Soft tissue fraction and vascular volume fraction were quantified. For determination of minimal voxels size for imaging of the morphology of small vessels, images were reconstructed at increasing voxel sizes.

Results: Quantitative micro-CT analysis showed a significant increase in the volume fraction of soft tissue in the fibrotic lungs compared to controls (p < 0.001). Specimens with lung fibrosis showed a significant reduction in vascular volume compared to controls (p < 0.02). Specimens with emphysema showed a significant decrease in soft tissue fraction (p < 0.001). Morphological differences in small vessels of fibrotic specimens disappear at voxel sizes larger than 115 µm.

Conclusions: Our findings indicate that micro-CT can characterize pathological

alterations of the human lung fine structure. The voxel resolution of current clinical CT scanners cannot be expected to visualize morphology of ultrastructural vascular alterations in vascular remodeling of fibrotic lungs.

P97

Oxygenation of human lung lesions as assessed by MR-BOLD measurement and the link to histopathology

Sedlacek O.L.¹, Reinmuth N.², Ley S.², Kauczor H.U.², Heussel C.P.², for the Heidelberg-Group of the Lungsysproject

¹Universitätsklinikum, Radiologische Klinik Abteilung Diagnostische und Interventionelle Radiologie, Heidelberg, Germany, ²Universitätsklinikum, Thoraxhospital & Diagnostische und Interventionelle Radiologie, Heidelberg, Germany

Purpose: Blood oxygenation and vascular function are considered important predictors in the growth of malignant tumours. BOLD MRI is able to visualize oxygen associated changes reflecting these parameters in thoracic tissues.

Material and methods: 46 patients (28 male, median age 66 ± 5 yrs) with suspicion of bronchial carcinoma (median size 3,5 ± 2,7 cm) underwent clinically indicated MRI prior to treatment. MRI was performed on a clinical 1.5T scanner (Avanto, Siemens). A BOLD sequence (TE 60ms) was included without a navigator run and acquired 150 continuous 3D data-sets of the whole lung (4 mm, isovoxel). The patient inspired either ambient air or 15l/min pure oxygen via a face mask ("block-design", 5 phases on/off oxygen). Evaluation was performed with SPM8 (Wellcome Department, London; standard procedures). Realignment in 3 planes, non-canonical hemodynamic response function (hrf). Histology was acquired in all patients either via biopsy or after resection.

Results: In 19 patients histology showed benign lesions with significant (p < 0.05) variation in the BOLD signal being detectable in 16 patients. In the patients with malign lesions there was significant variation in the BOLD signal in 22 of 27 cases. The amplitudes within the lung tumours showed a tendency towards lower oxygen dependent changes as compared to benign lesions.

Conclusion: BOLD MRI reflects oxygen-induced changes in human lung tumours not discriminating between dignity.

However, there might be typical response patterns of the BOLD signal in lung tumours predicting dignity.

P98

Multi-nuclear MRI investigations into V/Q matching

Wild J.M.¹, Marshall H.¹, Deppe M.H.¹, Capener D.¹, Parra-Robles J.¹, Rajaram S.¹, Parnell S.R.¹, Swift A.¹, Hillis S.¹, Billings C.², Hurdman J.³, Condliffe R.³, Elliot C.³, Kiely D.G.³, Lipson D.A.⁴, Lawson R.²

¹University of Sheffield, Unit of Academic Radiology, Sheffield, United Kingdom,

²University of Sheffield, Respiratory Medicine, Sheffield, United Kingdom, ³Sheffield



Teaching Hospitals NHS Trust, Pulmonary Vascular Disease Unit, Sheffield, United Kingdom, ⁴GlaxoSmithKline, King of Prussia, United States

Purpose: The matching of ventilation and perfusion in the lungs is essential for gas exchange, and measurement of regional ventilation and perfusion (V/Q) distribution is desirable for the assessment of lung function. The combination of ³He ventilation, ³He pO₂ (partial pressure of oxygen) and dynamic contrast enhanced (DCE) ¹H perfusion MRI was investigated as a means to assess V/Q matching using a radiation-free methodology. Preliminary experience in chronic obstructive pulmonary disease (COPD) and chronic thromboembolic pulmonary hypertension (CTEPH) patients is presented.

Methods: ³He ventilation, ³He pO₂, ¹H DCE perfusion and anatomical ¹H images were acquired from four COPD patients and two CTEPH patients at 1.5T.

Results: ³He ventilation and ¹H DCE perfusion images visualised regional V/Q distributions with high spatial resolution. Regions of elevated pO₂ corresponded to large perfusion deficits seen in the DCE perfusion images in some patients. In the future image registration will be used to in order to carry out a more thorough comparison between the DCE perfusion and the ³He images (both pO₂ maps and ventilation images). ³He pO₂ imaging is non-invasive and spatially matched to the ventilation data but is limited to ventilated regions. The V/Q visualisation offered by the ³He ventilation and ¹H DCE images is however encouraging.

Conclusions: Ventilation imaging, pO₂ mapping, and DCE perfusion imaging give complementary views of the ventilation and perfusion distributions in patients and are useful for assessment of V/Q matching in COPD and CTEPH.

Acknowledgements: Funded by GlaxoSmithKline (RES111175), UK EPSRC and CVBRU. GE for polariser support.

P99

Lung cancer screening by morphological MRI in comparison to low-dose CT - Initial results

*Tremper J.¹, Puderbach M.², Stieltjes B.¹, Eichinger M.¹, Schlemmer H.-P.¹, Delorme S.¹
¹German Cancer Research Center, Dep. of Radiology, Heidelberg, Germany, ²Thoraxklinik Heidelberg, Dep. of Diagnostic and Interventional Radiology, Heidelberg, Germany*

Purpose: Lung cancer screening with CT applies ionizing radiation. This is problematic in long-term follow-up with accumulating doses. The aim of this study was to examine the potential of magnetic resonance imaging (MRI) for the detection of suspected lung lesions in comparison to low-dose CT.

Methods: 23 participants of the Heidelberg lung cancer screening trial (LUSI) showing a suspicious lung lesion in CT that requires immediate workup received a non contrast lung MRI (HASTE, VIBE, TruFisp in coronal and transversal orientation). The study time was approx. 7 minutes. The MR data was checked for suspicious lesions. The results were compared to CT.

Results: 19 of the 23 suspicious lesions could be identified by MRI comparable to CT. 4 lung lesions could not be identified (1 of them being smaller than 8 mm; 2 of them localized in the costo-phrenical angle; 1 lesion had already resolved by the time the MRI was performed). In Fisher's Exact test independence can be rejected ($p = 0.11$), proving MRI being as accurate as CT in detecting relevant lung lesions.

Conclusion: These preliminary results show that morphological MRI of the lung is capable to detect suspicious lung lesions comparable to low-dose CT.

P100

Morphometric assessment of pulmonary airways in MDCT

Fetita C.L.^{1,2}, Ortner M.^{1,2}, Brillet P.-Y.^{3,4}, Grenier P.A.^{5,6}, Prêteux F.⁷

¹Telecom SudParis, ARTEMIS, Evry, France, ²CNRS UMR8145, MAP5, Paris, France,

³Université Paris 13, Paris, France, ⁴AP-HP, Avicenne Hospital, Bobigny, France,

⁵Université Pierre et Marie Curie, Paris, France, ⁶AP-HP, Pitié-Salpêtrière Hospital, Paris,

France, ⁷Mines ParisTech, Paris, France

Purpose: Introduce a computerized system for airway morphology quantitative assessment in asthma and COPD based on MDCT imaging.

Materials and methods: A computerized system is here developed for the investigation and follow-up of airway diseases based on routine MDCT acquisitions. It provides fully-3D and 2D cross-section measurements of the airway tree, with zero or limited user-interaction, based on the fully-automated segmentation of the 3D airway lumen and central axis computation (beyond sub-sub-segmental bronchi). An intuitive semi-quantitative estimation and colour-coded visualization of the lumen calibre is proposed, which allows a visual inspection of the airway morphology with feed-back on local narrowing or thickening. Such inspection is reinforced by an automatic detection and display of high likelihood regions of stenosis and bronchiectasis along the airway central axis. Cross-section quantification of lumen and wall areas, wall thickness and lumen-to-bronchus ratio is provided along any selected airway segment at the desired sampling interval, which ensures a near-volumetric analysis of bronchi and dense measurements able to capture the heterogeneity of the diseases throughout the lungs. The quantification of bronchus subdivision region is possible via a fully-3D segmentation of the inner and outer airway wall surfaces, with associated visualization routines.

Results: The developed system has been validated on simulated MDCT computer phantoms and successfully applied in two studies on moderate and severe asthma (96 and 30 cases respectively) showing high accuracy irrespective to the CT protocol used.

Conclusions: Three-dimensional quantitative analysis of airway lumen and wall in MDCT offers new insights in asthma and COPD.



P101

Calcified pulmonary nodules on chest radiographs: can we rely on radiologists' assessment?

Antunes V.B.¹, Meirelles G.S.P.¹, Szarf G.¹, Maciel R.P.¹, Figueiredo C.M.¹, Macedo-Neto A.C.¹, Piovesan A.C.¹, Jasinowodolinski D.²

¹Fleury Medicina e Saude, São Paulo, Brazil, ²Hospital do Coracao, São Paulo, Brazil

Purpose: The purpose of this exhibit is to determine accuracy of chest radiologists to detect calcifications in pulmonary nodules on analog and digital radiographs.

Material/Methods: Chest radiographs (analog and digital) of 91 consecutive patients in which pulmonary nodules had been detected were reviewed by seven chest radiologists, who assigned their confidence for presence of nodules and presence or absence of calcifications (1-certainty calcified, 2-possibly calcified, 3-possibly not calcified and 4-certainty not calcified). Multidetector computed tomography (CT) images of all patients were then reviewed for confirmation of lung nodules, presence and type of calcifications (benign or uncertain) and additional significant findings. CT images were used as gold standard for confirmation of nodules and presence of calcification.

Results: Chest radiographs had an accuracy of 73.3% for nodule detection, with low specificity (30%) and many false positive results (70%). Digital radiographs had good accuracy (87.5%) for detection of calcifications, significantly higher than analog radiographs (54.5%). The negative predictive value of chest radiograph for calcifications was low for digital (46.1%) and analog radiographs (23%) in comparison to CT. Three patients had other significant findings on CT (spiculated nodules or ground glass focal opacities) not demonstrated on radiographs. Fourteen (15.4%) patients had additional nodules > 0.5 cm on CT that had not been identified on radiographs.

Conclusion: Chest radiologists had good accuracy for detection of calcification in lung nodules on digital radiographs, but its negative predictive value was low.

P102

Pleural thickening: Pictorial essay of the main MDCT features

Maciel R.P.¹, Antunes V.¹, Figueiredo C.M.¹, Macedo Neto A.C.¹, Szarf G.¹, Meirelles G.¹

¹Fleury Medicina e Saude, Sao Paulo, Brazil

Purpose: To describe the main MDCT appearances of diseases characterized by pleural thickening.

Methods: The authors present sample cases of the main causes of pleural thickening, with emphasis on MDCT findings and differential diagnosis.

Results: The following conditions were selected:

1. Pleural plaques, which are the most common manifestation of asbestos exposure, usually bilateral, with a posterolateral predominance.
2. Localized pleural fibrous tumors

3. Lipomas, which usually have a uniform density and measure less than 50 HU on CT. Liposarcomas, which are typically larger, infiltrative, and symptomatic.
4. Diffuse thickening due to asbestos exposure, defined by some criteries: bilateral thickening involving at least 25% of the chest or 50% if unilateral; pleural thickness greater than 5 mm at any site; obliteration of the costophrenic angle.
5. Prior tuberculosis and traumatic empyema, which are responsible for diffuse pleural thickening with calcifications (fibrothorax).
6. Pleural metastatic disease, characterized by parietal pleural thickening greater than 1 cm, circumferential pleural thickening, nodular pleural thickening and mediastinal pleural thickening.
7. Malignant mesotheliomas, characterized by nodular pleural thickening, fissural involvement with pleural effusions and pleural calcification
8. Other rare primary tumors of the pleura, including sarcomas, usually manifesting as large masses.

Conclusion: Imaging plays an important role in the diagnosis and subsequent management of patients with pleural disease. The knowledge of the main findings of diffuse thickening on MDCT is crucial for a correct diagnosis.

P103

Evaluation of HRCT and VCT as longitudinal monitoring methods of lung tissue after irradiation in murine models

Dadrich M.¹, Peschke P.², Flechsig P.¹, Jenne J.², Kauczor H.-U.¹, Huber P.²

¹University Hospital Heidelberg, Department of Diagnostic and Interventional Radiology, Heidelberg, Germany, ²DKFZ, Radiation Oncology, Heidelberg, Germany

Purpose: Radiotherapy for lung cancer may induce severe pulmonary damage because radiation tolerance of lung tissue is limited. Invasive methods such as histological analysis are the goldstandard to monitor the changes in lung tissue in a murine model. Those methods, however, are not viable to repeatedly examine the lung of the one mouse in a longitudinal way to study the development of lung tissue over a period of time.

Here we investigated the feasibility and correctness of non-invasive radiological methods to monitor the effect of a single dose radiation to the thorax of mice.

Materials/Methods: Thoraces of C57BL/6 mice were irradiated with a single dose of 20 Gy using a high energy photon beam (6 MeV). Histological analysis and non - invasive radiological monitoring using Volume - CT and high resolution CT were performed before irradiation and 2, 12, 16, 20 and 24 weeks after irradiation.

Results: Histology showed that radiation induced severe pulmonary fibrosis in all mice such as thickening of alveolar membranes and extracellular collagen deposition. The first signs of fibrosis could be observed 12 weeks after irradiation, deteriorating up to the endpoint after 24 weeks. In accordance with histology, radiological data from VCT and HRCT showed increasing patchy, reticular abnormalities and in some cases ground glass opacities.



Conclusions: Our data suggest that HRCT and VCT data correlate well with histological analysis and thus are feasible and reliable methods to monitor changes in lungs of mice. Non-invasive radiological imaging can be used for the repeated examination of lungs in animal models.

P104

CT-Guided transthoracic breast lesion location wire implantation for small nonpalpable pulmonary nodules

Ilse B.¹, Vandembroucke F.¹, de Mey J.¹

¹Universitair Ziekenhuis Brussel, Radiology, Brussels, Belgium

Purpose: To evaluate the technique, safety and diagnostic reliability of transthoracic wire implantation for nonpalpable and invisible small pulmonary nodules (SPN) prior to video-assisted thoracoscopic surgery (VATS).

Methods: From April 2009 till January 2011, seventeen patients underwent 18 VATS resections after insertion of a 'breast lesion localization wire' (7,7 or 10,7cm needle length and 20-gauge size) into a SPN. The wire was placed using a CT fluoroscopy procedure. The patients were assessed with respect to localization and puncture of the lesion, duration and complication rate of the procedure, conversion thoracotomy rate during VATS and pathologic results.

Results: Preoperative CT-guided wire implantation succeeded in all patients. The average CT-guided procedure time was 12 min (range 8-15 min) and no complication was noted. There was no conversion to thoracotomy needed in any patient. Histological assessment revealed metastases in 11 patients, non-small-cell lung cancer in 4 patients, interstitial fibrosis in 2 patients and a sarcoid nodule in 1 patient.

Conclusions: Percutaneous CT-fluoroscopy guided wire placement is a useful and safe technique for localizing nonpalpable pulmonary nodules during VATS resection.

P105

Quantification of pulmonary perfusion using different regularization methods

Salehi Ravesh M.¹, Laun F.B.¹, Brix G.², Kuder T.A.¹, Puderbach M.³, Ley-Zaporozhan J.⁴, Ley S.⁴, Fieselmann A.⁵, Herrmann M.F.¹, Schranz W.⁶, Semmler W.¹

¹German Cancer Research Center, Division of Medical Physics in Radiology, Heidelberg, Germany, ²Federal Office for Radiation Protection, Department of Medical and Occupational Radiation Protection, Oberschleissheim, Germany, ³German Cancer Research Center, Division of Radiology, Heidelberg, Germany, ⁴University Hospital Heidelberg, Diagnostic and Interventional Radiology, Heidelberg, Germany, ⁵University of Erlangen-Nuremberg, Pattern Recognition Lab and Erlangen Graduate School in Advanced Optical Technologies (SAOT), Nuremberg, Germany, ⁶Faculty of Physics, University of Vienna, Physics of Functional Materials, Vienna, Austria

Purpose: Tissue microcirculation can be quantified by a deconvolution analysis of concentration-time courses measured by dynamic contrast-enhanced MRI. However, deconvolution is an ill-posed problem, which requires regularization of the solutions.

Materials: Four algebraic deconvolution methods were evaluated: Truncated singular value decomposition (tSVD) and generalized Tikhonov regularization (GTR) in combination with the L-curve-criterion (GTR-LCC), a modified LCC (GTR-MLCC), and a residue function model (GTR-RFM) that takes a-priori knowledge into account. To this end, DCE-data were simulated for different noise ratios (SNR) and measured at a 1.5-T-system in the lung of 10 healthy volunteers and 20 patients. Serial MR-images were acquired using a 3D-FLASH-sequence with combined parallel acquisition (GRAPPA) and view-sharing ($TR/TE/FA$, 1.92ms/0.81ms/40°; FOV=500'216 mm²; ST=4mm) with a temporal resolution of 1.6 s. The acquisition was started simultaneously with automatic administration of the contrast agent (0.05 mmol/kg-b.w. Gd-DTPA) followed by a saline flush of 30 ml with an injection rate of 5 ml/s in end-inspiratory breath-hold.

Results: In contrast to the established algorithms tSVD and GTR-LCC, GTR-MLCC and GTR-RFM yielded more reliable estimates of pulmonary tissue parameters. In the simulations, GTR-RFM had approximately the same accuracy as GTR-MLCC, but a slightly smaller precision at low SNRs. For SNR 20 the estimated pulmonary blood flow values estimated by both techniques deviates by less than 10 % from the true values. On the other hand, GTR-RFM proved to be more advantageous in case of measured patient data.

Conclusion: In conclusion, GTR-RFM is recommended for quantification of pulmonary microcirculation by algebraic deconvolution of DCE-MRI data.

P106

Differential diagnosis of non malignant pulmonary masses

Palacio D.¹, Betancourt S.L.¹, Godoy M.¹, Truong M.¹

¹University of Texas MD Anderson Cancer Center, Diagnostic Imaging, Houston, United States

Purpose: To describe the potential differential diagnosis of solitary pulmonary masses that resemble lung cancer, their etiology, histopathology features, and imaging appearance and therapeutic options.

Materials and methods: We display a wide variety of pathology proven cases of non lung cancer in patients presenting with lung masses, in our institution.

Results: The etiology of non-neoplastic pulmonary masses is extensive and includes congenital, infectious, inflammatory, vascular, occupational and benign neoplastic lesions.

Conclusion: In order to accurately characterize lung masses, the radiologist should be aware of the broad spectrum of potential etiologies, other than lung cancer, in the proper clinical setting.

**P107****Congenital Pulmonary Airway Malformation presenting as unilateral cystic lung disease: Evaluation by MDCT**Ghosh S.¹, McLoney E.¹¹The Ohio State University Medical Center, Radiology, Columbus, United States**Purpose/Aim:**

1. Review the imaging characteristic of Congenital Pulmonary Airway Malformation (CPAM) on 64 slice Multidetector Computed Tomography (MDCT).
2. Show CT and pathology correlation.

Content Organization:

1. Discuss etiology and clinical history related to Congenital Pulmonary Airway Malformation.
2. Show relevant histologic and imaging differences between this entity and other cystic lung diseases.
3. Discuss outcomes and followup.

Summary:

1. Understand the imaging findings related to an unusual presentation of Congenital Pulmonary Airway Malformation, previously not well described on radiology literature.
2. Understand that since the radiologic findings can sometimes be non-specific, clinical and pathology correlation is crucial.

P109**Distribution of CT-quantified emphysema in heavy smokers participating in a lung cancer screening trial: Association with lung function decline**Mohamed Hoesein F.A.A.¹, Zanen P.¹, van Ginneken B.², van Klaveren R.J.³, Prokop M.², Lammers J.-W.J.¹¹University Medical Center Utrecht, Division of Heart & Lungs, Department of Respiratory Medicine, Utrecht, Netherlands, ²Radboud University Nijmegen Medical Center, Department of Radiology, Nijmegen, Netherlands, ³Erasmus University Medical Center, Department of Respiratory Medicine, Rotterdam, Netherlands

Purpose: To assess the association between CT-quantified emphysema distribution (upper / lower lobe) and lung function decline in heavy current and former smokers participating in a lung cancer screening trial.

Material and methods: In this medical ethical approved study, 587 participants underwent CT-scanning of the lungs and pulmonary function testing at baseline and after a median (interquartile range) follow-up of 2.9 (2.8-3.0) years. The lungs were automatically segmented based on anatomically defined lung lobes. Severity of emphysema was automatically quantified per anatomical lung lobe and was expressed as the 15th percentile; (HU point below which 15% of the low attenuation voxels are

distributed (Perc15)). The emphysema distribution was based on principal component analysis. Linear mixed models, correcting for age, height, BMI packyears and smoking status, were used to assess the association of emphysema distribution and FEV₁/FVC-decline.

Results: Mean (SD) age was 60.2 (5.4) years, mean baseline FEV₁/FVC was 71.6 (9.0) % and overall mean Perc15 was -908.5 (20.9) HU. Participants with upper lobe predominant emphysema had a lower FEV₁/FVC after follow-up compared to participants with lower predominant emphysema (p=0.001), independent of the total extent of emphysema

Conclusion: Heavy current and former smokers with upper lobe predominant emphysema have a more rapid decrease in FEV₁/FVC than those with lower lobe predominant emphysema, independent of the overall extent of emphysema. These results seem to indicate that upper and lower lobe predominant emphysema may be different phenotypes.

P110**Phenotyping of obstructive lung disease based on MRI data: preliminary experience**U. Wolf¹, C. Hoffmann¹, N. Bojadzic¹, M. Terekhov¹, L.M. Schreiber¹, S. Triphan², A. Anjorin³, S. Ley³, S. Korn⁴, C. Taube⁴, K.K. Gast¹, K.T. Kreitner¹, C. Düber¹¹Department of Diagnostic and Interventional Radiology, University Hospital Mainz²Research Center Magnetic Resonance Bavaria³Department of Diagnostic and Interventional Radiology, University Hospital Heidelberg⁴ Pulmonary Department, University Hospital Mainz**Aims:**

To provide functional and structural information based on MRI data. In a first step to investigate the day-to-day repeatability of proton-MRI data compared to pulmonary function test (PFT) parameters in Asthma and COPD patients.

Methods:

10 patients were enrolled (Asthma n=5; COPD n=5) age span 50-70years; FEV1 > 40% ; MRI scans were run on a 1.5 T scanner (Siemens, Avanto); patients were examined on 2 consecutive days: first pulmonary function tests were performed; after that, a proton-MRI thorax protocol including morphology, respiratory dynamics; ventilation, perfusion both prior to and during the inhalation of O₂ was applied.

Results:

Both, PFT and MRI were well tolerated by the patients. Median test-re-test variabilities were found as follows: (i) FEV1 < 10%, (ii) T1 < 3%, (iii) max. vertical diaphragm excursion Δr < 20%.

Conclusion:

As only half of the patients have been enrolled, the findings are preliminary. Our results suggest a good repeatability of FEV1 and T1, respectively. As for the parameter "diaphragm excursion" a significant amount of variability may be due to varying motivation of the patient. This is a well-known phenomenon in lung function testing.



For Your Notes

Lined area for notes on page 78, featuring 21 horizontal orange lines.

For Your Notes

Lined area for notes on page 79, featuring 21 horizontal orange lines.

www.ESTI2011.org